An innovative decentralized strategy for I-AUVs cooperative manipulation tasks

An innovative decentralized strategy for I-AUVs cooperative manipulation tasks

R. Conti, E. Meli, A. Ridolfi, B. Allotta

University of Florence
Department of Industrial Engineering (DIEF)
Via di Santa Marta 3, 50139 - Florence, Italy
Corresponding author: roberto.conti@unifi.it

Interuniversity center of
Integrated Systems for the Maritime Environment (ISME)
www.isme.unige.it

Abstract

In the last years, a challenging field of autonomous robotics is represented by cooperative mobile manipulation carried out in different environments (aerial, terrestrial and underwater environment). As regards cooperative manipulation of Intervention-Autonomous Underwater Vehicles (I-AUVs), this application is characterized by a more complex environment of work, compared to the terrestrial or aerial ones, both due to different technological problems, e.g. localization and communication in underwater environment. However, the use of Autonomous Underwater Vehicle (AUV) and I-AUV will necessarily grow up in the future exploration of the sea. Particularly, cooperative I-AUVs represent the natural evolution of single centralized I-AUV because they may be used in various underwater assembly tasks, such as complex underwater structure construction and maintenance (e.g. underwater pipeline and cable transportation can be carried out by multiple cooperative I-AUVs). Furthermore, underwater search and rescue tasks could be more efficient and effective if multiple I-AUVs were used.
In this paper, the authors propose an innovative decentralized approach for cooperative mobile manipulation of I-AUVs. This decentralized strategy is based on a different use of potential field method; in particular, a multi-layer control structure is developed to in parallel manage the coordination of the swarm, the guidance and navigation of the I-AUVs and the manipulation task. The main advantage of the potential field method is that less information are necessary: navigation and control problems are reduced to the evaluation of the distance vector among the vehicles, object and obstacles. Moreover, because of the technological problems caused by the underwater environment, the reduction of the transmitted data is one of the keypoints of this architecture. In MATLAB®-Simulink®, the authors have simulated a transportation task of a partially known object along a reference trajectory in an unknown environment, where some obstacles are placed. The task is performed by a I-AUV swarm composed of four vehicles, each one provided of a 7 Degrees Of Freedom (DOFs) robotic arm.

Keywords: Intervention-Autonomous Underwater Vehicle, Decentralized control strategy, Cooperative mobile manipulation, Potential Field Method, Underwater Robotics

1. Introduction

Cooperative mobile manipulation represents a challenging field for autonomous robotics (Figure 1), especially in the underwater environments. Both in the military, in the industrial and in the academic fields, the coordinated control of multiple mobile manipulators (with one or more robotic arms) have attracted many economic interests [4],[5]. The great benefit in such systems stems from the capability of carrying out complex and dexterous tasks which cannot be simply made using a single manipulator: for instance, multiple cooperative manipulators can be used to move objects, action that cannot be performed by a single robot (due to the object size and weight constraints). In aerial and terrestrial applications, the strategies for cooperative mobile manipulation can be addressed dividing the approach into different tasks; these tasks are performed in parallel to complete the cooperative manipulation task.

- Swarm motion planning and control: in literature there are different approaches to the guidance, navigation and control of the swarm. Conceptually, these approaches may be divided in centralized and decentralized architectures. Decentralized approaches are mainly based on the distributed control techniques in terms of controllers and sensors, such as Consensus

http://dx.doi.org/10.1016/j.robot.2015.06.006

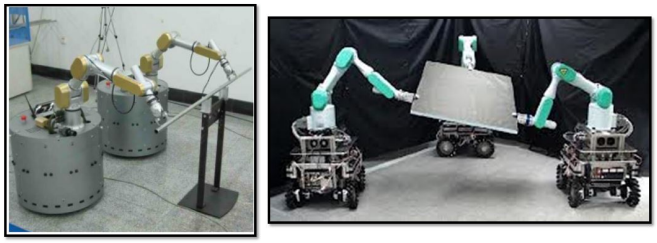

Figure 1: Application of Cooperative Mobile Manipulation for terrestrial robots and for I-AUVs

based approaches [1] or Feedback-Linearization based approaches [2] [7]; there are also applications of potential field methods (just few examples are related to the underwater environment [32]). The main drawbacks of these methods are the less accuracy and robustness in terms of controller tasks; instead, the suitable advantages are the limited information transmitted and the reduced computational time. On the contrary, centralized approaches are usually based on the leader-follower architecture [17],[18] in which a vehicle has more information and sensors (the leader), and the follower group blindly executes the leader motion. However, the use of centralized approaches supposes many problems in terms of communication towards the less-equipped vehicles, in addition to a higher cost of the leader vehicle. The advantage is the great accuracy and robustness in terms of controller.

- Vehicle motion planning and control: in the single vehicle motion planning different approaches are used, i.e. trajectory tracking or path-following approaches [19], [20]. As regards the control strategies, linear or non-linear control laws [19] can be considered.

- Manipulator motion planning and control: the robotic arm motion planning is usually performed through kinematic or dynamic control strategies [3]; in this case many combined control architectures involving in parallel (force and position) control of the robotic arm are developed [11], [12], [13].

Each task of cooperative mobile manipulation applications introduces different issues mainly depending on the goals to be achieved and on the environment. Compared to the analysis of the general state of the art of cooperative mobile manipulators, cooperative manipulation of Intervention-Autonomous Underwater Vehicles (I-AUVs) represents a more complex field of application, compared to the terrestrial or aerial ones, both due to different technological problems (e.g. localization and communication in underwater environment) and to the lack of an accurate knowledge in the modelling of fluid-vehicle interaction. Many reasearch projects deal with the development of I-AUV such as TRIDENT [29] and PANDORA [30] (Figure 2), mainly because the use of AUV and I-AUV will necessarily grow up in the future exploration of the sea. ***In this scenario, despite of the strong gap between cooperative manipulation and real sea operations, cooperative I-AUVs represent the natural evolution of centralized I-AUVs because they may be used in various underwater assembly tasks, such as complex underwater structure construction and maintenance (e.g. underwater pipeline and cable transportation can be carried out by multiple cooperative I-AUVs). Furthermore, underwater search and rescue tasks could be more efficient and effective if multiple I-AUVs are used [17].***

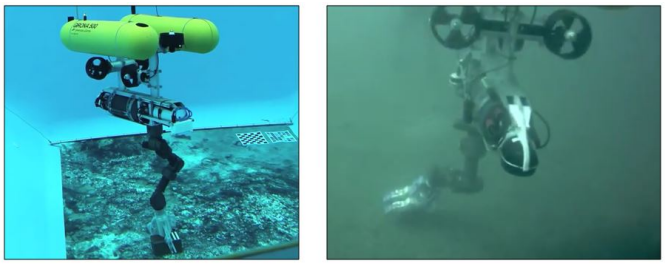

Figure 2: Intervention-AUV developed in the framework of the EU project TRIDENT (pool test and sea test)

Also in cooperative mobile manipulation of I-AUVs, the same three tasks have to be performed in parallel to complete the manipulation operations:

- Swarm motion planning and control: I-AUVs swarm motion planning and control have been analysed in detail in few research works [5], [15]. Currently, the main research and economic investments have been made on the motion planning of AUV [8], [31] both in centralized and in decentralized approaches[33], [34]; in particular, many research efforts are carried out in the cooperative localization and communication [21].

- Vehicle modelling, motion planning and control: modelling of I-AUVs can be found in [6],[9], [10] and [8]. In [11], a control law to track a desired motion trajectory for an I-AUV has been proposed, where an observer has been designed to provide velocity estimation. In [20], a navigation strategy based on path following approach is presented. In [9],[15] feedback linearization control has been proposed for an I-AUV, where the exact dynamic model is assumed to be known. In [16], the I-AUV control scheme compensates the non linear coupling effects.

- Manipulator motion planning and control: as regards the robotic arm, several force control schemes have been presented in [12], [13] and [8]. In [14], a solution to the redundancy resolution problem and motion coordination between vehicle and manipulator by using fuzzy technique has been presented.

According to the presented literature, few projects involving the cooperative mobile manipulation of I-AUVs

in underwater environments are currently on going, due to the technological and economical issues. In the previous state of the art analysis, most of the presented approaches present complex and heterogeneous solutions for the three parts: swarm, vehicle and robotic arm motion planning and control. The authors propose to improve the state of the art through an innovative decentralized approach for cooperative mobile manipulation of I-AUVs, completely based on potential field method [3], [32], able to realize a homogeneous and less complex solution for the three parts. This decentralized strategy is based on a different use of potential field method; particularly, a multi-layer control structure is developed to in parallel manage the coordination of the swarm, the guidance and navigation of I-AUVs and the manipulation task. This homogeneous and decentralized solution allows the reduction of communication problems and of computational resources. The multi-layer control structure controls both the swarm, the vehicle and the robotic arm motion. The main layers of the structure are:

- Vehicle-Vehicle interaction: the main aim of this part are the guidance of the swarm and the avoidance of the impact between vehicles. The required inputs are the vehicle distances and the swarm position in the world reference frame. To estimate these distances, a suitable acoustic localization algorithm is developed.
- Vehicle-Object interaction: this part supports the kinematic control of the robotic arm to properly manipulate the object, able to modify the trajectory of the vehicle to help the manipulation task, in parallel maintaining the required distance between vehicle and object. The required inputs are the joint coordinates, measured through joint sensors.
- Vehicle-Environment interaction: this is the classical use of the potential field method for the obstacle avoiding. The required inputs are the distance vectors between the vehicles and the obstacles, estimated by means of acoustic or optic devices (e.g. multibeam device or cameras).
- Object-Environments interaction: the object-environment interaction is naturally obtained through the knowledge of the object and of the obstacles (obtained by the previous layers) and it is necessary to avoid the collisions among the object and the obstacles.

The main advantage of the potential field method is that less information are necessary in terms of distances, relative positions and velocities among the vehicles, object and obstacles; therefore, this approach allows the reduction of the on board sensors and of the computational load, reducing the whole system complexity. Moreover, because of the technological problems caused by the underwater environment, the reduction of the transmitted data is one of the keypoints of this architecture. As regards the vehicle localization, the swarms usually use complex localization algorithms and redundant expensive sensors (e.g. Ultra Short Base Line, USBL) [26][27]; the innovative concept is to use the object to be manipulated (supposed to be partially known a priori) such as a swarm reference system and the surface vehicle only as connection point with the world reference system. This way, the architecture allows the use of a single USBL device placed on the surface vehicle and of acoustic modems to localize the swarm I-AUVs [28]: the approach may be defined decentralized because the knowledge of the I-AUV is limited to the on board sensor data and to few exchanged data (distances only). In addition, no supervisor vehicle is necessary to complete the task, because each component of the swarm has a sufficient knowledge of the group and does not need to communicate with the surface vehicle.
Because of the gap between the real operations of the AUVs and the cooperative mobile manipulation of I-AUVs, the authors decided to evaluate the cooperative manipulation strategy only in terms of numerical simulations. However, thanks to experience acquired in previous research activities [42], [45], [46], [47], [43], [44] in the AUV field, the authors have modelled the typical behaviour of the sensors (e.g. USBL, Inertial Measurement Unit, Echosouder, etc..) to better investigate the accuracy of the method with respect to the sensors performances. The authors, in MATLAB®-Simulink®, have simulated this approach with an I-AUV swarm composed of 4 vehicles, each one provided of a 7 Degree Of Freedoms (DOFs) robotic arm. The simulation scenario is the transportation of a partially known object in an unknown environment, e.g. a harbour; particularly, the manipulation task is to carry the object along a desired trajectory where some obstacles are placed.
The research paper is organized as follows: in section 2 the cooperative mobile manipulation strategy is explained in detail, and the main potential fields and the communication architecture are described. In section 3, a description of the I-AUV kinematical and dynamic models is given; finally, in section 4 the numerical results of the cooperative manipulation task are widely discussed.

2. Cooperative mobile manipulation strategy

In this section, the innovative control architecture for cooperative mobile manipulation tasks of I-AUVs is presented. This control architecture deals with two separate problems: the simultaneous control of the swarm, vehicle and robotic arm, and the underwater localization. The I-AUV swarm (Figure 3) consists of four I-AUVs supported by an external vehicle (e.g. a Remotely Operated Surface Vehicle, ROSV). The ROSV is used to geo-localize the swarm through a classical GPS system and to communicate with the I-AUVs swarm using an USBL; the transmitted data is uniquely the position of a one of the vehicles in

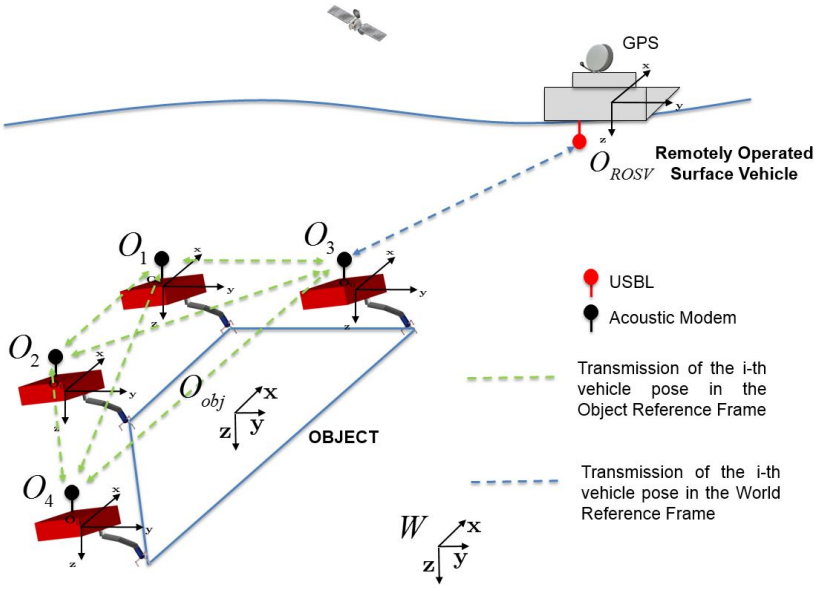

Figure 3: General architecture of the swarm

the World Reference Frame. I-AUV swarm vehicles communicate to each others the relative poses in the Object Reference Frame by means of simple acoustic modems; therefore, that approach is completely decentralized one in which the localization is performed only using few on board sensors and where the distance vectors are calculated in the object reference frame (no master vehicle is necessary).

2.1. Potential field multi-layer architecture

The control architecture of the swarm for cooperative mobile manipulation tasks is based on the development of a control framework able to manage in parallel the guidance of the swarm, the navigation of the vehicles and the manipulation of the object. In literature, several approaches involving heterogeneous controls of vehicle-manipulator systems (where the controls of the three subjects are managed separately) especially developed for terrestrial or aerial applications are presented [1], [2]. The main drawbacks in using these approaches in underwater environments are related to the lack of reliable low-cost localization systems, to the issues involving acoustic communication methods and to the use of heterogeneous control techniques. Therefore, the authors propose a novel control architecture completely decentralized to overcome the localization and communication problems in underwater environment but with a homogeneous control strategy to control in parallel the three tasks (swarm guidance, vehicle navigation and object manipulation) based on the potential field method.
In particular, potential field methods are usually employed to control vehicles in unstructured environments where the generation of the vehicle trajectories cannot be made a priori, e.g. when some obstacles are present; furthermore, these techniques are mainly based on the estimation of the distance vectors. The proposed control architecture applied to I-AUVs swarm introduces the usage of the potential field method not only in the trajectory generation in unstructured environments but also in the manipulation tasks and in the swarm control. The approach may be defined fully decentralized in terms of communication and localization issues because of the knowledge of each vehicle is limited to few on board sensors necessary for the evaluation of the distance vectors.
In the potential field method, the vehicles are considered as particles immersed in a potential field generated both by the goal and by the obstacles. The goal generates an attractive potential and each obstacle generates a repulsive one. Consequently, the I-AUVs immersed in the potential field are subjected to these two contributes: the target force action that drives to the goal (due to the attractive potential gradient generated by the goal) and the obstacle force actions that repulse the vehicles from the obstacles (due to the repulsive potential gradient produced by the obstacles). As regards the advantages of the potential field method, it is based only on the distance vector estimation and the exact knowledge of the vehicle position in the world reference frame is not necessary. For the analysis of the cooperative mobile manipulation architecture, some hypotheses have been made:

- the object shape and the connection points between vehicle and object are known (estimated using acoustic and optical sensors);
- the I-AUV control points the vehicle in the attractive target direction;
- the approaching phase to the object is not considered: a kinematic constraint, simulating a fixed connection, is defined between the gripper and the object.

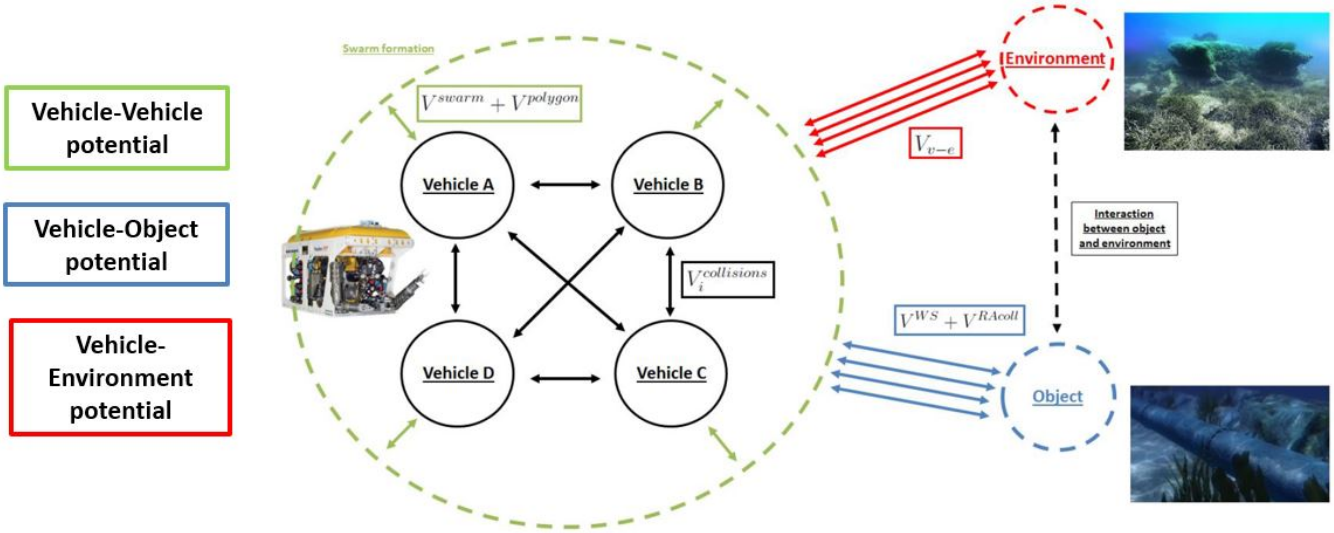

Figure 4: Interactions among potentials

In Figure 4, the interactions between vehicles, object and environment are shown. The control architecture involves three different subjects: vehicles, object and environment, and it is based on the interactions among different potentials:

- Vehicle - Vehicle (green): the interactions between vehicles consist of two different contributes, i.e. maintaining the swarm formation and avoiding vehicle collisions with other vehicles. The inputs are the vehicle distances and the swarm position in the world reference frame. To estimate these distances, a suitable acoustic localization algorithm is developed.

- Vehicle - Object (blue): the interactions between vehicles and the object to be manipulated are in blue and the four arrows show the connections between vehicles and object. The required inputs are the joint coordinates, measured by joint sensors.

- Vehicle - Environment (red): the interactions between the vehicles and the environment (obstacles) are coloured in red and the four arrows indicate the interactions with vehicles. The required inputs are the distance vectors between the vehicles and the obstacles; a suitable acoustic devices for obstacle individuations is necessary.

- Object - Environment (black dotted line): this interaction is implicitly obtained by other potentials; it is a secondary task obtained as a consequence of the knowledge both of the object shape and of the obstacle one (estimated by sensors).

In the following sections, the considered potentials are explained in details.

2.1.1. Vehicle-Vehicle potential

The Vehicle-Vehicle potential V_{v-v} consists of three main parts: the attractive potential to keep the vehicles in formation (i.e. swarm inside a sphere, useful to the cooperative manipulation), the repulsive potential to keep the vehicles in a predefined shape (e.g. vertices of a regular polygon) and the repulsive potential to avoid collisions between vehicles. The forces acting on the i-th vehicles (for $i = 1, .., n$ and n=number of vehicles) are:

$$\vec{F}_{v-v,i} = \vec{\nabla} V_{v-v,i}, \tag{1}$$

with

$$V_{v-v,i} = V_i^{swarm} + V_{i,j}^{polygon} + V_{i,j}^{collisions} \tag{2}$$

where $V_{v-v,i}$ is the total Vehicle-Vehicle potential acting on the i-th vehicle (for $i = 1, .., n$), V_i^{swarm} is the vehicle swarm potential, $V_{i,j}^{polygon}$ is vehicle polygon potential (where $j = 1, ..n$ and $j \neq i$) and $V_{i,j}^{collisions}$ is the vehicle collision potential (where $j = 1, ..n$ and $j \neq i$). In Figure 5, the main contributes due to these potentials are schematized as a function of the distance d. The vehicle swarm potential is based on the attractive potential and it is carried out both to keep within a spherical shape the I-AUVs (useful for the cooperative manipulation) and to attract the vehicles to the target position. In this case, in the world reference frame (defined with the pedix ^{W}), the considered distance $\vec{d}_i^W = \vec{\eta}_i^W - \vec{G}_d^W(t)$ is the distance between the vehicle position $\vec{\eta}_i^W$ and the center of the spherical shape $\vec{G}_d^W(t)$ (which represents the desired trajectory of the swarm). Therefore, the force $\vec{F}_i^{swarm}$ acting on the

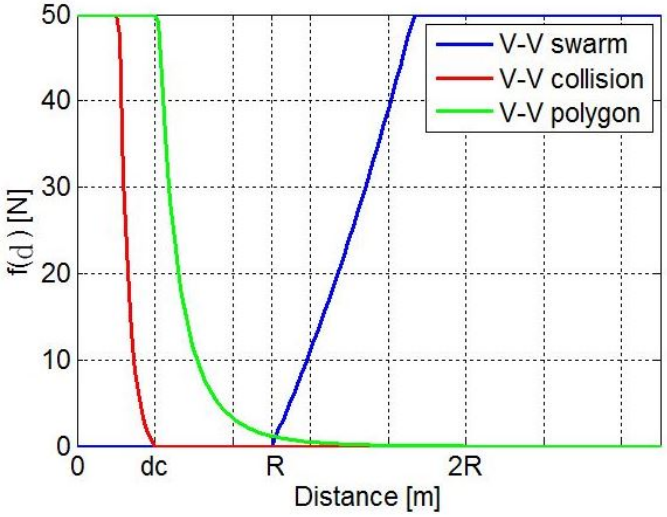

Figure 5: Vehicle-Vehicle characteristic functions

vehicle is:

$$\vec{F}_i^{swarm} = \vec{\nabla} V^{swarm} = -f^{swarm}\left(\left\|\vec{d}_i^W\right\|\right)\frac{\vec{\eta}_i^W - \vec{G}_d^W(t)}{\left\|\vec{\eta}_i^W - \vec{G}_d^W(t)\right\|} \tag{3}$$

where $f^{swarm}\left(\left\|\vec{d}_i^W\right\|\right)$ is a defined function of the distance. In this case, the function has to consider a low boundary equal to the radius R of the spherical shape in order to attract the vehicle outside the shape and to keep free the inside vehicles:

$$f^{swarm}\left(\left\|\vec{d}_i^W\right\|\right) = \begin{cases} k_s\left(\left\|\vec{d}_i^W\right\| - R\right)^2 \\ \left\|\vec{d}_i^W\right\| \geq R \\ \\ 0 \\ \left\|\vec{d}_i^W\right\| < R \end{cases}, \tag{4}$$

where k_s is the shape parameter to increase the slope of the curve.
The attractive potential is a vector field proportional to the difference $\vec{\eta}_i^W - \vec{G}_d^W(t)$ that points at $\vec{G}_d^W(t)$. The vehicle polygon potential $V^{polygon}$ is a repulsive potential and its objective is to keep the vehicles at the vertices of a regular polygon (depending on the number of vehicles) that can be useful for the cooperative manipulation. In this repulsive potential, the distance to be considered is the reciprocal distance among two vehicles $\vec{d}_{i,j}^W = \vec{\eta}_i^W(t) - \vec{\eta}_j^W(t)$ where $\vec{\eta}_i^W$ is the $i-th$ vehicle position and $\vec{\eta}_j^W$ is the $j-th$ vehicle position (in this case, the positions are time variable). Therefore, the force $\vec{F}_{i,j}^{polygon}$ acting on the $i-th$ vehicle is the sum of the contributes for each vehicle:

$$\begin{aligned} \vec{F}_{i,j}^{polygon} &= \vec{\nabla} V^{polygon} = \\ &= f^{polygon}\left(\left\|\vec{d}_{i,j}^W\right\|\right)\frac{\vec{\eta}_i^W(t) - \vec{\eta}_j^W(t)}{\left\|\vec{\eta}_i^W(t) - \vec{\eta}_j^W(t)\right\|} \end{aligned} \tag{5}$$

where $f^{polygon}\left(\left\|\vec{d}_{i,j}^W\right\|\right)$ is a characteristic function of the distance. This case, the repulsive function has to consider an upper bound equal to the $2x$ the spherical shape radius to not overcome the spherical surface and to keep on the edge the vehicles:

$$f^{polygon}\left(\left\|\vec{d}_{i,j}^W\right\|\right) = \begin{cases} +k_p\left(\frac{1}{\left\|\vec{d}_{i,j}^W\right\|^2} - \frac{1}{4R^2}\right), \\ \left\|\vec{d}_i^W\right\| < 2R \\ \\ 0 \\ \left\|\vec{d}_i^W\right\| \geq 2R \end{cases}, \tag{6}$$

where k_p is the repulsive shape parameter to increase the slope of the curve.
Finally, the vehicle collision potential $V_i^{collisions}$ is a repulsive potential and prevents collisions between the vehicles. This potential is calculated for each vehicle and is useful when the object to be transported is quite small compared to the vehicle workspaces and the risk that vehicle collisions may occur. Also in this potential, the distance to be considered is the reciprocal distance among two vehicles $\vec{d}_{i,j}^W = \vec{\eta}_i^W(t) - \vec{\eta}_j^W(t)$, described before. The force $\vec{F}_{i,j}^{collisions}$ acting on the $i-th$ vehicle is the sum of the contributes for each vehicles:

$$\begin{aligned} \vec{F}_{i,j}^{collisions} &= \vec{\nabla} V_{i,j}^{collisions} = \\ &= f^{collisions}\left(\left\|\vec{d}_{i,j}^W\right\|\right)\frac{\vec{\eta}_i^W(t) - \vec{\eta}_j^W(t)}{\left\|\vec{\eta}_i^W(t) - \vec{\eta}_j^W(t)\right\|} \end{aligned} \tag{7}$$

where $f^{collisions}\left(\left\|\vec{d}_{i,j}^W\right\|\right)$ is a characteristic function of the distance. The repulsive function considers an upper bound equal to a threshold d_c of $2x$ the vehicle sizes.

$$f^{collisions}\left(\left\|\vec{d}_{i,j}^W\right\|\right) = \begin{cases} +k_c\left(\frac{1}{\left\|\vec{d}_{i,j}^W\right\|^2} - \frac{1}{d_c^2}\right), \\ \left\|\vec{d}_i^W\right\| < d_c \\ \\ 0 \\ \left\|\vec{d}_i^W\right\| \geq d_c \end{cases}, \tag{8}$$

where k_c is the repulsive shape parameter to increase the slope of the curve.
In Table 1, all the parameters associated to the Vehicle-Vehicle potentials are reported.

2.1.2. Vehicle-Object potential

The Vehicle-Object potential V_{v-obj} allows the motion of the vehicle to maintain a correct position of the end-effector with respect to the vehicle position. Particularly, as it can be seen in Figure 6 there are three different important intervals in terms of distance between the end effector and the vehicle ($\vec{d}_{ee,v}^W = \vec{\eta}_v^W - \vec{\eta}_{ee}^W$): the first one ($0 \leq d_{ee,v}^W < WS_{min}$) defines a repulsive action to reduce the possibility of a collision between the end-effector and

Table 1: Vehicle-Vehicle potential

Parameter	Value
R	$5\ m$
k_s	$10\ N/m^2$
$2R$	$10\ m$
k_p	$0.1\ Nm^2$
d_c	$2\ m$
k_c	$1.5\ Nm^2$

the vehicle; the second one ($WS_{min} \leq d^W_{ee,v} < WS_{max}$) is an area where the potential actions are not enabled because, in this part, the classical kinematic controller technique is used; finally, in the third part ($d^W_{ee,v} \geq WS_{max}$) an attractive action to move the vehicle towards the robotic arm workspace is implemented (when the vehicle is away from the objectworkspace). The workspaces WS_{min} and WS_{max} define respectively the minimum accepted distance and the maximum accepted one between the end-effector and the vehicle. The vehicle-object action could be applied using both the vehicle thrusters or the joint actuators. In the proposed approach, the vehicle-object potential is supposed to act on the vehicle motion; this way, the motor thrusts can be better exploited. The vehicle-object potential consists of two contributes: the workspace potential function V^{WS} and the robotic arm collision potential function V^{RAcoll}. These two contributes can be identified through a suitable curve limited with upper and lower bounds respectively defined by the maximum extension of the robotic arm and by the minimum one:

$$V_{v-o} = V^{WS} + V^{RAcoll} \tag{9}$$

where V_{v-o} is the whole Vehicle-Object potential acting on the vehicle, V^{WS} is the workspace potential, which permits to maintain the end-effector position within the robotic arm workspace, and V^{RAcoll} is the robotic arm collision potential avoiding collisions among vehicle and end-effector (see Figure 6). The workspace potential is based on the attractive potential function and is necessary to maintain the end-effector position within the workspace of the robotic arm. As regards the considered distance, $\vec{d}^W_{ee,v} = \vec{\eta}^W_v - \vec{\eta}^W_{ee}$ is the distance between the robotic arm position $\vec{\eta}^W_v$ and the end-effector position $\vec{\eta}^W_{ee}$. The force $\vec{F}^{WS}_i$ acting on the vehicle is:

$$\vec{F}^{WS} = \vec{\nabla} V^{WS} = -f^{WS}\left(\left\|\vec{d}^W_{ee,v}\right\|\right) \frac{\vec{\eta}^W_v - \vec{\eta}^W_{ee}}{\|\vec{\eta}^W_v - \vec{\eta}^W_{ee}\|}, \tag{10}$$

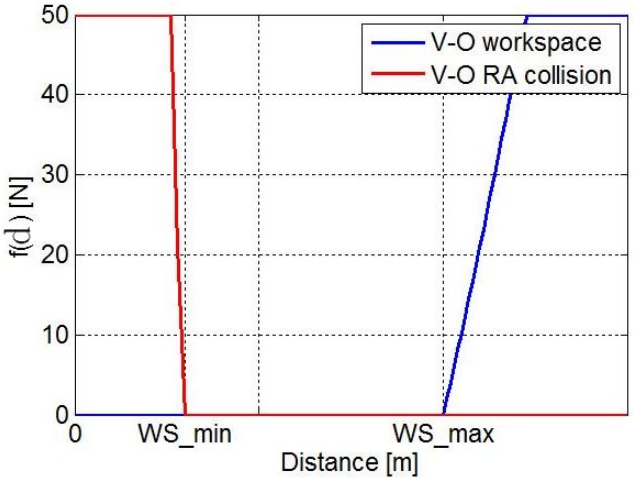

Figure 6: Vehicle-Object characteristic functions

where $f^{WS}\left(\left\|\vec{d}^W_{ee,v}\right\|\right)$ is a characteristic function of the distance,

$$f^{WS}(\left\|\vec{d}^W_{ee,v}\right\|) = \begin{cases} -k_{WS}\left(\left\|\vec{d^W_{ee,v}}\right\| - WS_{max}\right)^2 \\ for\ \left\|\vec{d^W_{ee,v}}\right\| \geq WS_{max} \\ \\ 0 \\ for\ \left\|\vec{d^W_{ee,v}}\right\| < WS_{max} \end{cases}, \tag{11}$$

where k_{WS} is the shape parameter to increase the slope of the curve.
The attractive potential is a vector field proportional to the difference $\vec{\eta}^W_v - \vec{\eta}^W_{ee}$ that points away from $\vec{\eta}^W_{ee}$. The robotic arm collision potential is instead a repulsive potential and its aim is to keep the end-effector away from the vehicle (avoiding undesired collisions). This potential is required to change the vehicle trajectory when the manipulator is moving in a different position and may be dangerous for the vehicle. In this repulsive potential, the distance to be considered is the same of the previous case: $\vec{d}^W_{ee,v} = \vec{\eta}^W_v - \vec{\eta}^W_{ee}$. The force $\vec{F}^{RAcoll}$ acting on the vehicle is:

$$\vec{F}^{RAcoll} = \vec{\nabla} V^{RAcoll} = f^{RAcoll}\left(\|d^W_{ee,v}\|\right) \frac{\vec{\eta}^W_v - \vec{\eta}^W_{ee}}{\|\vec{\eta}^W_v - \vec{\eta}^W_{ee}\|}, \tag{12}$$

where $f^{RAcoll}\left(\left\|\vec{d}^W_{ee,v}\right\|\right)$ is a characteristic function of the distance. The repulsive function has an upper bound equal

Table 2: Vehicle-Object potential

Parameter	Value
WS_{max}	0.8 m
k_{WS}	100 N/m^2
$WS_{\min}$	0.4 m
k_{RA}	100 Nm^2

to the minimum extension of the robotic arm:

$$f^{\text{RAcoll}}(\left\|\vec{d}^{W}_{ee,v}\right\|) = \begin{cases} +k_{RA}\left(\frac{1}{\left\|\vec{d}^{W}_{ee,v}\right\|^2} - \frac{1}{WS^2_{min}}\right) \\ for \ \left\|\vec{d}^{W}_{ee,v}\right\| < WS_{\min} \\ \\ 0 \\ for \ \left\|\vec{d}^{W}_{ee,v}\right\| \geq WS_{\min} \end{cases}, \tag{13}$$

where k_{RA} is the repulsive shape parameter to increase the slope of the curve. In Table 2, all the parameters associated to the Vehicle-Object potentials are reported.

2.1.3. Vehicle-Environment potential

The Vehicle-Environment potential V_{v-e} is necessary to avoid obstacles during the transportation of the object. This potential is a repulsive potential because it has to modify the vehicle trajectories to avoid obstacles. The Vehicle-Environment potential V_{v-e} is calculated for each obstacle. In this potential, the distance to be considered is the reciprocal distance between a vehicle and the obstacle $\vec{d}^{W}_{i,o} = \vec{\eta}^{W}_{i}(t) - \vec{\eta}^{W}_{o}(t)$ where $\vec{\eta}^{W}_{i}$ is the $i-th$ vehicle position and $\vec{\eta}_o$ is the obstacle position. The force $\vec{F}^{v-e}_{i,o}$ acting on the $i-th$ vehicle is the sum of the contributes of each obstacle:

$$\vec{F}^{v-e}_{i,o} = \vec{\nabla} V_{v-e} = +f^{v-e}_{i,o}\left(\left\|\vec{d}^{W}_{i,o}\right\|\right)\frac{(\vec{\eta}^{W}_{i}(t) - \vec{\eta}^{W}_{o}(t))}{\left\|\vec{\eta}^{W}_{i}(t) - \vec{\eta}^{W}_{o}(t)\right\|}, \tag{14}$$

where $f^{v-e}_{i,o}\left(\left\|\vec{d}^{W}_{i,o}\right\|\right)$ is a characteristic function of the distance. The characteristic function is:

$$f^{v-e}_{i,o}(\left\|\vec{d}^{W}_{i,o}\right\|) = +k_O\left(\frac{1}{\left\|\vec{d}^{W}_{i,o}\right\|^2} - \frac{1}{d^2_O}\right), \tag{15}$$

where k_O is the repulsive shape parameter to increase the slope of the curve. In Table 3, all the parameters associated to the Vehicle-Environment potentials are reported.

2.1.4. Object-Environment interaction

The Object-Environment interaction is useful to guarantee the safety of the manipulated object during the transportation phase. This interaction is obtained as a consequence of the effects of the previous potentials: the Vehicle-Environment potential allows the obstacle avoidance but, considering also the size of the object to be manipulated, it can be used also to keep safe the object itself. The proposed approach may also be extended introducing a specific Object-Environment potential V_{obj-e}.

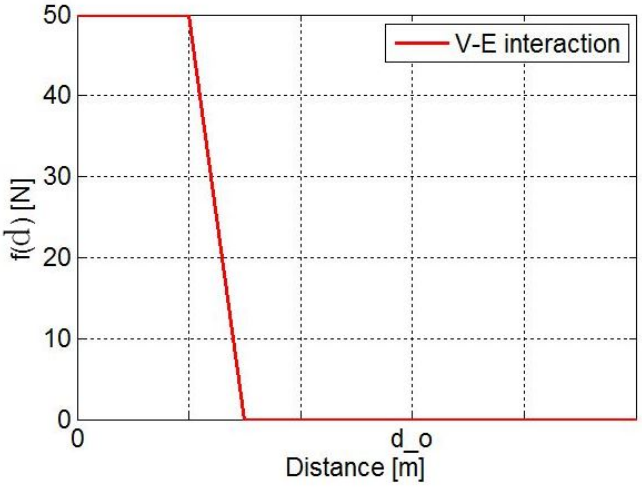

Figure 7: Vehicle-Environment characteristic function

Table 3: Vehicle-Environment potential

Parameter	Value
d_O	16 m
k_O	10 Nm^2

2.2. Distance estimation algorithm

In this section, the description of the swarm localization strategy is given in details. Usually, swarm localization strategies in underwater environment are based on expensive sensors (e.g. Long Base Line, LBL, or Ultra Short Base Line, USBL) and on complex localization algorithms to provide the proper position of each vehicle in the world reference frame [26], [28]. The main drawback of the current approaches is mainly related to the low frequency of the vehicle position update (due to the characteristics of the sensors): however, this characteristics is unacceptable for cooperative manipulation tasks in which the position update should have a higher frequency to obtain correct control actions. Therefore, the authors have developed an innovative localization strategy mainly based on internal sensors (IMU, cameras, joint sensors, acoustic sensors) with high frequency rate in order to overcome this problem: in fact, on board sensors firstly provide the position of the vehicle in the object reference frame, and then, through the localization algorithm, the reciprocal distances of the vehicles in the world reference frame for the maintaining of the swarm formation and the execution of cooperative manipulation tasks.

Table 4: Distance vectors

N	**Distance vector**	**Potential functions**	**Equation**
I	Distance between I-AUVs	$V_i^{collisions}$-$V^{polygon}$	$\vec{d}_{i,j}^{W} = \vec{\eta}_{vi}^{W}(t) - \vec{\eta}_{vj}^{W}(t) = R_{IMU}^{Ti} R_{DKi}^{T} \vec{d}_{i,j}^{obj}$
II	Distance between I-AUVs and the swarm sphere	V^{swarm}	$\vec{d}_{i}^{W} = \vec{\eta}_{vi}^{W} - \vec{G}_{d}^{W}(t)$
III	Distance between I-AUV (i-th) and end effector (i-th)	V^{WS}-V^{RAcoll}	$\vec{d}_{ee,v}^{W} = \vec{\eta}_{vi}^{W} - \vec{\eta}_{ee,i}^{W} = R_{IMU}^{i}(\vec{d}_{v,i}^{V} + \vec{d}_{DKi}^{V})$
IV	Distance between i-th vehicle and obstacle	V_{v-e}	$\vec{d}_{i,o}^{W} = \vec{\eta}_{i}^{W}(t) - \vec{\eta}_{o}^{W}(t) = R_{IMU}^{i} \vec{d}_{obs}^{V}$

As described before, the authors propose an innovative solution, completely decentralized, to carry out cooperative mobile manipulation tasks uniquely based on distance vector estimations. Before describing distance evaluation, it is necessary to define all the reference frames and the physical quantities involved in the distance estimation algorithm. The distance estimation algorithm is used by each vehicle for the calculation of its potentials; the potentials are calculated only by means of the on board sensors. In particular, as shown in Table 4, $\vec{\eta}_{vi}^{W}$ is the position of the i-th vehicle, $\vec{G}_{d}^{W}(t)$ is the central position of the swarm circle, $\vec{\eta}_{ee,i}^{W}$ is the position of the end-effector of the i-th vehicle and $\vec{\eta}_{o}^{W}$ is the central position of the obstacle (all expressed in the world reference frame).

The proper evaluation of the distance vectors is necessary to calculate the potentials among the I-AUVs. The proposed architecture is conceived to reduce the data flow among the underwater vehicles and the ROSV to increase the reliability of the control architecture. The main idea to avoid expensive localization devices or complex communication architecture is to employ the manipulated object such as a local reference system of the swarm. Thus, through the hypotheses of partially known object and known connection points between I-AUVs and object (which are realistic ones, according to the current state of the art in the field of underwater mobile manipulation [3], [8]), the distance vectors are easily accessible; internal sensors of the vehicle, e.g. joint sensors, cameras, Inertial Measurement Unit (IMU), echosounder with a high data-flowrate, provide the correct pose of the I-AUV in the object reference frame.

The coordinates express in the world reference frame and introduced before (Table 4) must be now rewritten in local reference frames to be evaluated by means of internal sensors.

The distance estimation algorithm based on the object reference frame concept is in detail explained into Figure 8. The algorithm uses two different time scales: a long time interval $\Delta T = 5 - 10$ s obtained by the acoustic communication with the ROSV, and a short time interval $\Delta t = 0.1$ s, depending on the internal sensors (e.g. joint sensors, IMU and camera). The first contribute defines the update time of the data coming from outside the swarm; in particular, ΔT is the time interval between the calculation of the swarm potential functions and the re-updating of the

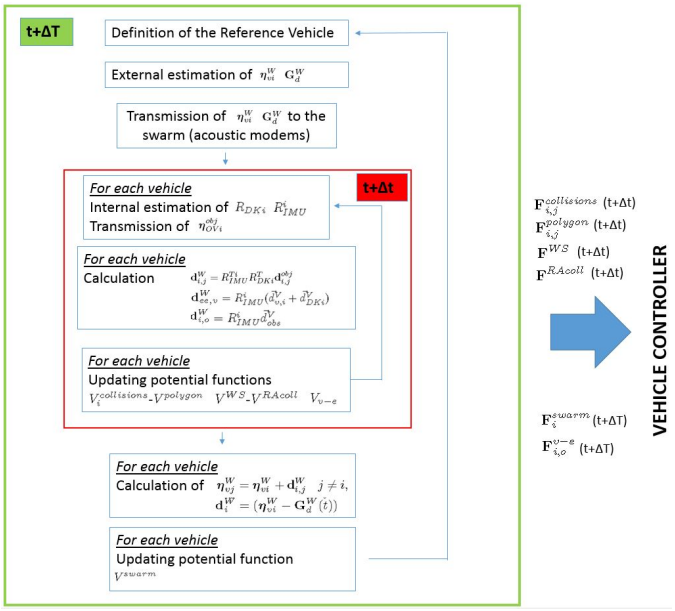

Figure 8: Distance estimation algorithm

reference vehicle position in the world reference frame. Instead, the second contribute is the update time of the data coming from inside the swarm; Δt is the time interval between the calculation of the potential functions involving the manipulation task and the re-updating of the vehicle positions in the object reference frame. The use of these two time scales is imposed to perform manipulation tasks and to decentralize the cooperative manipulation strategy from swarm external data.

According to Figure 9, a world reference frame $\vec{O}_W$, an i-th vehicle reference frame $\vec{O}_{vi}$ and an object reference frame $\vec{O}_{obj}$ are defined. Two rotation matrices R_{IMU}^{i} and R_{DKi}, respectively between the reference systems placed in $\vec{O}_W$ and $\vec{O}_{vi}$ and between the reference systems placed in $\vec{O}_{vi}$ and $\vec{O}_{obj}$ are expressed. In particular, R_{IMU}^{i} may be obtained only through an on board IMU measuring the vehicle orientation (by means of Euler angles e.g. ϕ_V,θ_V,ψ_V), and R_{DKi} is calculated by means of the direct kinematic model of the robotic arm (obtained measuring the joint coordinates). Supposing the rigid connection between the end-effector and the object, the orientation of the end-effector is the same of the object. The distance

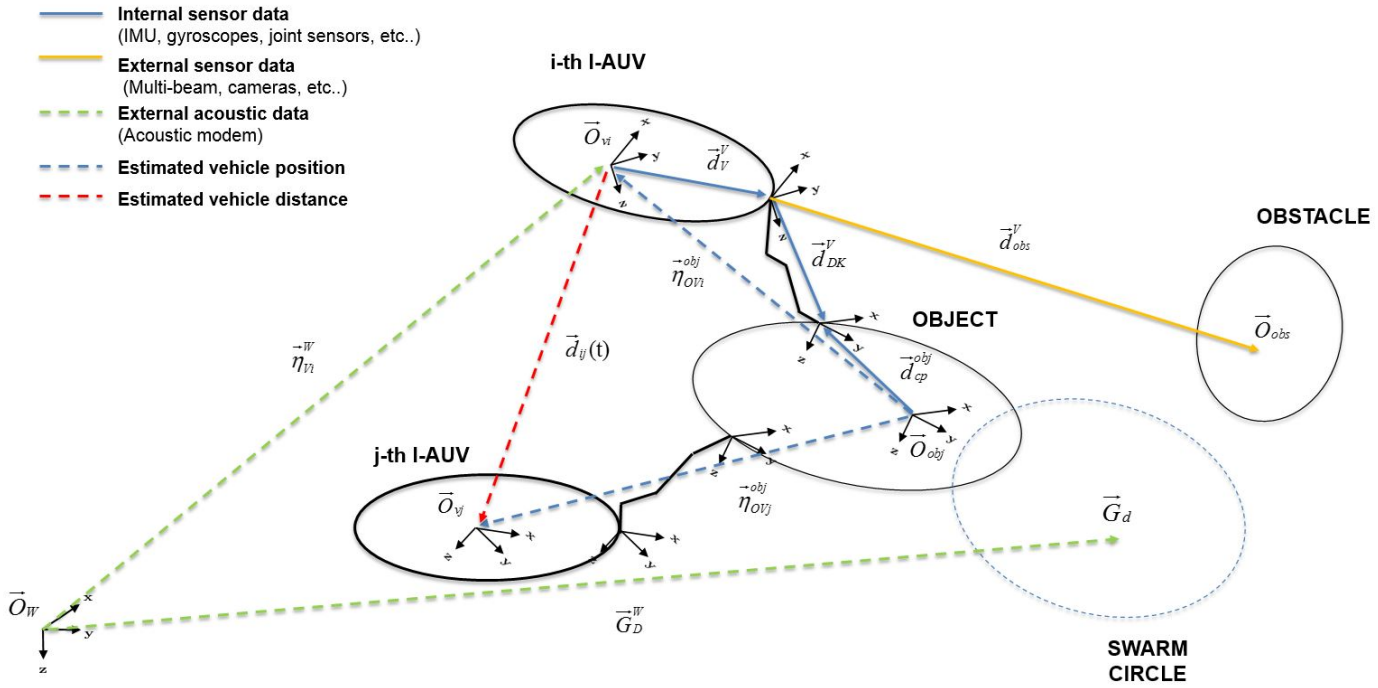

Figure 9: Distance vectors: data flows

vectors calculated into the world reference frame and described in Table 4 will be rewritten into the vehicle reference frame (in order to be expressed in terms of measured variables) and described as follows:

1. Ist distance (the distance among vehicles $\vec{d}^W_{i,j}$): rewriting the position of the i-th vehicle in the object reference frame O^W_{obj}, it is possible to obtain:

$$\vec{\eta}^{obj}_{OVi} = \vec{d}^{obj,i}_{cp} + R_{DKi}\vec{d}^V_{DKi} + R_{DK,i}\vec{d}^{V,i}_V; \qquad (16)$$

where $\vec{d}^{obj,i}_{cp}$ is the known position of the connection point in the object reference frame (being known by the constrain position), $\vec{d}^V_{DKi}$ is the position of the end-effector written in the manipulator base reference frame (due to the direct kinematics model obtained measuring the joint coordinates) and $\vec{d}^{V,i}_V$ is the position of the manipulator base written in the vehicle reference frame (known a priori). Through equation 16, it is possible to describe the position of the I-AUVs in the object reference frame; therefore, distance vectors $\vec{d}^{obj}_{i,j}$ can be obtained by the following equation:

$$\vec{d}^{obj}_{i,j} = \vec{\eta}^{obj}_{OVi} - \vec{\eta}^{obj}_{OVj}, \qquad (17)$$

which can be rewritten in the world reference frame:

$$\vec{d}^W_{i,j} = R^{Ti}_{IMU}R^T_{DKi}\vec{d}^{obj}_{i,j}. \qquad (18)$$

Equation 18 is completely decentralized because the positions of other I-AUVs are based on on-board data and local vehicle positions in the object reference frame (transmitted by means of acoustic modems). Positions of I-AUVs in the object reference frame $\vec{\eta}^{obj}_{OVi}$, for i= $1, 2, .., n_{vei}$ with n_{vei} equal to the number of vehicles, are transmitted among the vehicles by means of acoustic modems. The communication protocol exchanges vehicle positions every second, starting from the 1-st vehicle.

2. IInd distance (distance between I-AUVs and the swarm sphere $\vec{d}^W_i$): this distance cannot be calculated into the vehicle reference frame, therefore it is necessary that each vehicle finds its position into the world reference frame. The algorithm uses the distance calculated in the previous step $\vec{d}^W_{i,j}$ and the position into the world reference frame of one vehicle of the swarm; thus, knowing the absolute position of one vehicle and the distance from this one, the vehicle is able to recalculate its position into the world reference frame by Equation 19. For the position in the world reference frame, the algorithm needs that an I-AUV, which can be any of the swarm vehicles, receives its position $\vec{\eta}^W_{vi}$ (provided by the Remotely Operated Surface Vehicle and measured through USBL device) and that this information be transmitted to the rest of the swarm using:

$$\vec{\eta}^W_{vj} = \vec{\eta}^W_{vi} + \vec{d}^W_{i,j} j \neq i, for j = 1, 2...n_{vei}. \qquad (19)$$

The central position of the swarm $\vec{G}^W_d(t)$ is the desired position directly transmitted through the acoustic modems. This data is obtained by equation 20

with a relatively low time rate:

$$\vec{G}_d^W(t) = \vec{\eta}_{ROSV}^W + \vec{G}_{d-ASV}^W(t), \tag{20}$$

where $\vec{\eta}_{ROSV}^W$ is the ROSV world position acquired by the GPS and $\vec{G}_{d-ROSV}^W(t)$ is the desired position of the swarm written with respect to the surface vehicle (ROSV). Therefore, $\vec{d}_i^W$ is obtained as $\vec{\eta}_{vi}^W - \vec{G}_d^W(t)$.

3. IIIrd distance (distance between the i-th vehicle and the i-th end-effector $\vec{d}_{ee,v}^W$): this distance in the world reference frame can be easily calculated using physical quantities described into the vehicle reference frame using Equation 21:

$$\vec{d}_{ee,v}^W = R_{IMU}^i(\vec{d}_{v,i}^V + \vec{d}_{DKi}^V) \tag{21}$$

where $\vec{d}_{v,i}^V$ is the distance of the manipulator base into the vehicle reference frame (fixed and known a priori), R_{IMU}^i is the rotation matrix between world and vehicle reference frames (calculated by the internal IMU) and $\vec{d}_{DKi}^V$ is the distance vector due to the direct kinematics calculated measuring the joint variables.

4. IVth distance (distance between the i-th vehicle and the obstacle $\vec{d}_{i,o}^W$): the distance calculated into the vehicle reference frame $\vec{d}_{obs}^V$ is directly obtained by the on board sensors (multibeam echosounder or cameras) and can be easily transformed into the world reference frame (Equation 22)knowing the rotation matrix between world and vehicle reference frames R_{IMU}^i .

$$\vec{d}_{i,o}^W = R_{IMU}^i \vec{d}_{obs}^V \tag{22}$$

3. Modelling and control of the I-AUVs swarm

The I-AUVs swarm consists of n-th homogeneous I-AUVs, each of them equipped with a 7DOFs robotic arm.

3.1. AUV and robotic arm models

The I-AUV dynamic model is built through multibody techniques [24] and can be analysed dividing the study in two parts: the vehicle and the robotic arm. The geometrical and physical data regarding both the vehicle and the manipulator are taken from the technical literature; in particular, as regards the characteristics of the vehicle, they are based on [22], [23] and synthesised in Table 5. As regards the gripper, in this research work, the authors have supposed to simplify the connection with the object with a rigid connection. The models are completely developed in MATLAB®- Simulink®. According to the SNAME notation [19], the kinematic model of the AUV is defined in terms of $\vec{\eta}$ and $\vec{\nu}$ vectors. $\vec{\eta}$ represents the position ($\vec{\eta}_1$) and the orientation ($\vec{\eta}_2$) written in the fixed reference frame $< n >$; $\vec{\nu}$ components are respectively the linear ($\vec{\nu}_1$) and the angular ($\vec{\nu}_2$) speeds described into the body

Table 5: I-AUV characteristics

Characteristic	Value
Degree of Freedoms	6
Length	≈ 0.8 m
Breadth	≈ 0.6 m
Height	≈ 0.4 m
Mass in air	≈ 150 kg

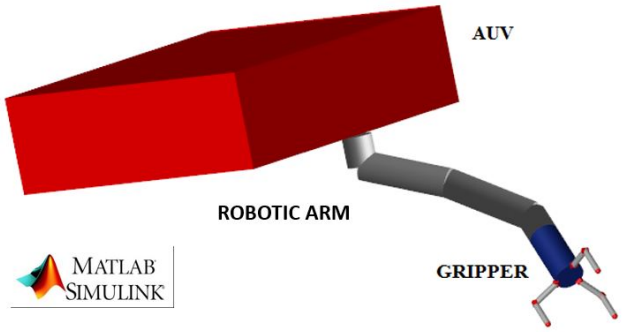

Figure 10: Model of the I-AUV

reference frame $< b >$ (both the fixed and the body reference frames use the NED directions). Vector $\vec{\tau}$ represents the linear forces ($\vec{\tau}_1$) and the torques ($\vec{\tau}_2$) applied to the vehicle as to the body reference frame $< b >$. The rela-

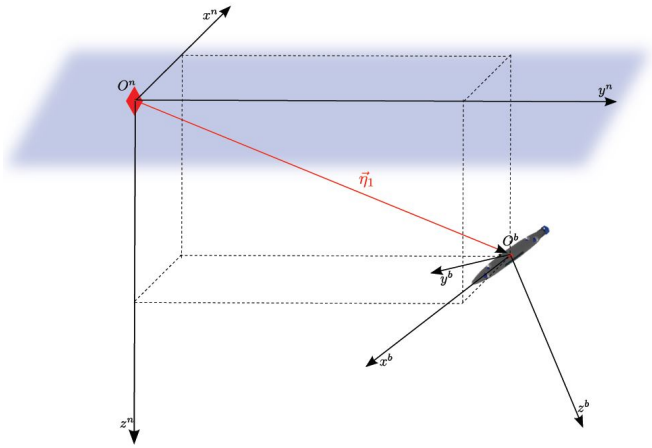

Figure 11: Reference systems of the I-AUV

tions between $\dot{\vec{\eta}}$ and $\vec{\nu}$ can be written using the following expression:

$$\dot{\vec{\eta}} = J_b^n(\vec{\eta}_2)\ \vec{\nu}\ , \tag{23}$$

where

$$J_b^n(\vec{\eta}_2) = \begin{bmatrix} R_b^n(\vec{\eta}_2) & 0_{3\times3} \\ 0_{3\times3} & T_b^n(\vec{\eta}_2) \end{bmatrix}. \tag{24}$$

Through (23), the kinematic equations describing the AUV model are:

$$\begin{aligned} \dot{\vec{\eta}} &= J_b^n\, \vec{\nu} \qquad\qquad \Leftrightarrow \quad \vec{\nu} = J_b^n \ ^{-1}\, \dot{\vec{\eta}} \\ \ddot{\vec{\eta}} &= J_b^n\, \dot{\vec{\nu}} + \dot{J}_b^n\, \vec{\nu} \quad \Leftrightarrow \quad \dot{\vec{\nu}} = J_b^n \ ^{-1}\, \left(\ddot{\vec{\eta}} - \dot{J}_b^n J_b^n \ ^{-1} \dot{\vec{\eta}}\right) . \end{aligned} \tag{25}$$

According to the literature [19], the dynamic equation of the vehicle is defined as follows:

$$M_{RB}(\vec{\nu})\dot{\vec{\nu}} + C_{RB}(\vec{\nu})\vec{\nu} = \vec{\tau}_H(\vec{\nu}, \vec{\nu}_C) + \vec{g}(\vec{\eta}) + \vec{\tau}_m + \vec{\tau}_{arm}, \tag{26}$$

where $M_{RB}(\vec{\nu})$ represents the mass matrix of the vehicle and $C_{RB}(\vec{\nu})$ is the Coriolis and centrifugal effect matrix. $\vec{g}(\vec{\eta})$, $\vec{\tau}_m$ and $\vec{\tau}_{arm}$ are respectively the contribution due to the gravity effects, the motor torques and the reaction forces of the robotic arm. From the classical equation of motion for an underwater vehicle [19], using the absolute velocity $\vec{\nu}$ written in the body reference frame and the current velocity $\vec{\nu_C}$, the following expression for $\vec{\tau}_H(\vec{\nu}, \vec{\nu}_C)$ can be obtained:

$$\begin{aligned} \vec{\tau}_H = & -M_A \dot{\vec{\nu}} + C_{RB}\left(\vec{\nu}\right)\vec{\nu}_c + \\ & + C_{RB}\left(\vec{\nu}_c\right)\vec{\nu}_r + C_{RB}\left(\vec{\nu}_c\right)\vec{\nu}_c + \\ & - C_A\left(\vec{\nu}\right)\vec{\nu}_r - D\left(\vec{\nu}\right)\vec{\nu}. \end{aligned} \tag{27}$$

where M_A is the added mass matrix due to the fluid viscosity, C_A is the Coriolis and centrifugal added effects, D is the damping matrix.
The I-AUV is provided of a robotic arm with 7 DOFs installed on the bow of the vehicle, in the middle of its lower part. For the kinematic model of the robotic arm (Figure 12), the joint coordinates $\vec{q} = [q_1\ q_2\ ..q_7]^T$ and the end-effector pose $\vec{x} = [x\ y\ z\ \phi\ \theta\ \psi]^T$ are defined. According to the Denavit-Hartenberg (D-H) approach, Table 6 collects the D-H parameters extracted for this robot.

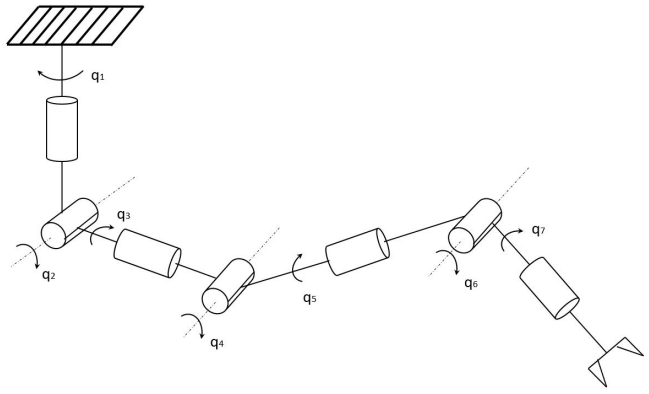

Figure 12: Kinematic scheme of the robotic arm

The main kinematic equations used to entirely describe the redundant manipulator are respectively, for the direct kinematics and for the differential kinematics:

$$T_n^0 = T_n^0\left(\vec{q}\ ,\right) \tag{28}$$

Table 6: Denavit-Hartenberg parameters

Link	a_i	α_i	d_i	ϑ_i
1	0	$\pi/2$	d_1	ϑ_1
2	0	$\pi/2$	0	$\vartheta_2 + \frac{\pi}{2}$
3	0	$-\pi/2$	d_3	ϑ_3
4	0	$\pi/2$	0	$\vartheta_4 + \frac{\pi}{2}$
5	0	$-\pi/2$	d_5	ϑ_5
6	0	$\pi/2$	0	ϑ_6
7	0	0	d_7	ϑ_7

$$\vec{v}_e = \begin{bmatrix} \dot{\vec{p}}_e \\ \vec{\omega}_e \end{bmatrix} = J\dot{\vec{q}} \tag{29}$$

where $T_n^0 \in \mathbb{R}^{4x4}$ is the homogeneous transformation matrix between the base reference frame $< 0 >$ fixed to the AUV and the end-effector reference frame $< n >$ and $\vec{q} \in \mathbb{R}^{7x1}$ is the joint variables, $\dot{\vec{p}}_e$ is the time derivative of the end-effector pose and $\dot{\vec{q}}$ is the time derivative of the joint coordinates $\vec{q}$. According to the literature [3], the redundant DOFs are used in the Closed Loop Inverse Kinematics method to solve secondary tasks (i.e. the avoidance of the singularity or the minimization of the kinetic energy).
The dynamic model of the robotic arm is simulated through the multibody techniques described before, where each rigid body is modelled as follows:

$$M_l^i(\vec{\nu})\dot{\vec{\nu}}_l^i + C_l^i(\vec{\nu}_l^i)\vec{\nu}_l^i = \vec{\tau}_H^i(\vec{\nu}_l^i, \vec{\nu}_{lC}^i) + \vec{g}^i(\vec{\eta}_l^i) + \vec{\tau}_l^i + \vec{\tau}_{mot}^i, \tag{30}$$

where $M_l^i(\vec{\nu})$ represents the mass matrix, $C_l^i(\vec{\nu}_l^i)$ is the Coriolis and centrifugal effect matrix of the i-th link. $\vec{g}^i(\vec{\eta}_l^i)$, $\vec{\tau}_{mot}^i$ and $\vec{\tau}_l^i$ are respectively the contributions related to the gravity effects, the actuation torques and the reaction forces due to the interaction with the other links of the robotic arm. As described before, the hydrodynamic effects $\vec{\tau}_H^i(\vec{\nu}_l^i, \vec{\nu}_{lC}^i)$ are calculated as:

$$\begin{aligned} \vec{\tau}_H^i = & -M_{Al}^i(\vec{\nu})\dot{\vec{\nu^i}} + C_l^i\left(\vec{\nu^i}\right)\vec{\nu^i}_c + \\ & + C_l^i\left(\vec{\nu^i}_c\right)\vec{\nu^i} + C_l^i\left(\vec{\nu^i}_c\right)\vec{\nu^i}_c + \\ & - C_{Al}^i\left(\vec{\nu^i}\right)\vec{\nu^i} - D^i\left(\vec{\nu^i}\right)\vec{\nu^i}. \end{aligned} \tag{31}$$

where $M_{Al}^i(\vec{\nu})$ is the added mass matrix due to the fluid viscosity, C_{Al}^i is the Coriolis and centrifugal added effects, D^i is the damping matrix. The geometrical and physical characteristics of the robotic arm are taken from the technical literature [22] and can be synthesised into the following parameters described in Table 7. The modelling of hydrodynamic and buoyancy effects $\vec{\tau}_H(\vec{\nu}, \vec{\nu}_C)$ both of the vehicle and of the robotic arm is strongly necessary to reproduce in a proper way the I-AUV dynamical behaviour during a navigation phase or a manipulation task. In particular, the authors have implemented these actions in each body belonging to the I-AUV system (vehicle, links of the arm and gripper); the simulated effects are:

Table 7: Robotic arm characteristics

Characteristics	Value
Links' length	d_1=d_3=d_5=d_7=0.3 m
Links' diameter	d_l=0.2 m
Links' mass	$m_l \approx 10$

Table 8: Object characteristics

Characteristics	Value
Longitudinal length	1.75 m
Breadth	4 m
Height	1 m
Hydrostatic effect due to the Archimede's law	Negative

- hydrostatic effects due to the added masses;
- hydrodynamic effects due to the added masses;
- drag and lift forces;
- buoyancy effects.

Assuming that the arm does not move at high velocities, the added mass matrix M_A and the matrix of the centrifugal and Coriolis effects C_A are respectively described in [19]. The coefficients of these matrix are obtained through a Computational Fluid Dynamics (CFD) simulation campaign considering, for each body, different velocities $\vec{\nu}$ and accelerations $\dot{\vec{\nu}}$, with the aim of building suitable and accurate look up tables to be used during the simulations.

As regards the modelling of object to be transported, Eq. 26 and Eq. 27 respectively describe the equation of motion of the object and the hydrodynamic contributes (Table 8). The mass and the inertia tensor have been evaluated according to its size and shape in order to obtain a negative object in water (which means that the volume of the moved water is less than the object own weight). The hydrodynamic parameters have been selected from literature [19] and they are referred to a non-hydrodynamic shape with high values of drag and lift coefficients.

3.2. AUV and robotic arm controls

The cooperative control architecture described in the previous section has to be merged in the whole I-AUV control architecture to improve the numerical robustness and the easiness of the approaches. The architecture is based on a multi-layer approach in which different contributes, coming from the different potentials, are combined with the classical control techniques to improve the robustness of the controller. In particular, two different controllers can be defined: vehicle controller Figure 13 and robotic arm controller Figure 14. The vehicle can be controlled using different strategies: position control on the 6 DOFs $(x, y, z, \alpha, \beta, \psi)$ using the PID approach or force control using the potential approach (on the x-y-z directions). The first approach can be useful for the approaching phase of the I-AUV to the object (precise positioning). The second one merges the control on the x-y-z directions in terms of forces with a PID strategy in terms of angular quantities α, β, ψ during cooperative manipulation tasks. Through the H matrix, which defines the relations $\vec{\tau} = H\vec{S}$ between vehicle forces $\vec{\tau}$ to be produced by the thrusters and thrusts $\vec{S}$ [19], the computed generalized forces obtained by the potentials in the vehicle reference frame are converted into the corresponding thrusts.

The robotic arm controller is based on the Closed Loop

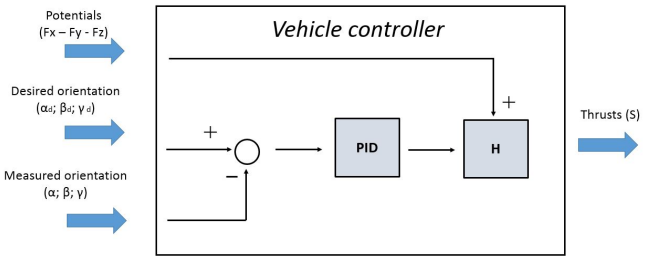

Figure 13: Vehicle controller based on potential approach

Inverse Kinematic approach in order to exploit redundant DOF of the manipulator. Particularly, once the desired

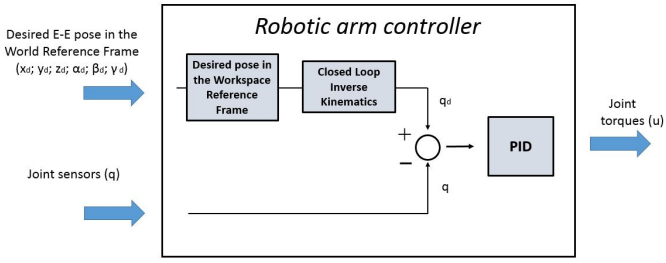

Figure 14: Robotic arm controller

end effector velocity $\vec{v}_e$ and the Jacobian J are given, it is desired to find the solutions $\dot{\vec{q}}$ satisfying the linear Equation (29) and minimizing the quadratic cost functional of joint velocities. The problem can be solved through the Lagrange multipliers method [3]:

$$\dot{\vec{q}} = J_r^{\dagger}\vec{v}_e, \tag{32}$$

where

$$J_r^{\dagger} = J^T(JJ^T)^{-1}, \tag{33}$$

is the right pseudo-inverse of Moore-Penrose [3]. The obtained solution locally minimizes the norm of the joint velocities. Supposing $\dot{\vec{q}}$ a solution of (29); then also $\dot{\vec{q}} + N_J\dot{\vec{q}}_o$

is a solution of N_J is a projector of the vector $\dot{\vec{q}}_o$ in the null space of J.

$$\dot{\vec{q}} = J_r^{\dagger}\vec{v}_e + (I_n - J_r^{\dagger}J)\dot{\vec{q}}_0. \tag{34}$$

The solution of this equation is composed of two terms: the first one is relative to the minimum norm joint velocities, and the second one, is the homogeneous solution. This solution satisfies the additional constrain. A direct consequence is that in case of $\vec{v}_e = 0$ is possible to generate internal motions that reconfigure the manipulator structure without changing the end effector pose.
The $\dot{\vec{q}}$ satisfy the equation (29) and are very close to $\dot{\vec{q}}_0$. In literature, there are many possible choices of $\dot{\vec{q}}_0$ and one of these is:

$$\dot{\vec{q}}_0 = k_0 \left(\frac{\partial w(\vec{q})}{\partial \vec{q}} \right)^T , \tag{35}$$

where $k_0 > 0$ and $w(\vec{q})$ is a secondary objective function of the joint variables. Since the solution moves along the direction of the gradient of the objective function, it attempts to maximize it locally compatible to the primary objective. In the I-AUV control objective function $w(\vec{q})$ is the following:

$$w(\vec{q}) = \sqrt{det(J(\vec{q})J^T(\vec{q}))}, \tag{36}$$

which vanishes at a singular configuration; thus, by maximizing this measure, redundancy is exploited to move away from singularities.
The inversion of the differential kinematics very close to a singularity can create many problems in terms of computational load. Therefore, it is useful to improve the robustness of the Jacobian J (or $J_r^{\dagger}$) a damped least squares inverse, defined as:

$$J^{\star} = J^T(JJ^T + k^2 I)^{-1}, \tag{37}$$

where $k^2 I$ is the the damping factor that renders the inversion better conditioned from a numerical viewpoint.

3.3. AUV sensor modelling

The mathematical models used to describe and simulate the functioning of the AUV on board sensors are here described. In particular, the authors have focused their interest on the sensors needed for the distance estimation involved in the cooperative manipulation algorithm (such as the USBL, the acoustic modem and the IMU). These sensors are typical for ROVs and AUVs: e.g. they are some of the ones mounted on the Typhoon class AUV [35], [36], developed and built by the University of Florence in the framework of the THESAURUS project. For the cooperative control architecture some of them have been modelled using the real features and performance to increase the accuracy of the proposed algorithm with respect to real scenario conditions.

3.3.1. Evologics® S2CR 18/34 Modem & USBL

In the distance estimation algorithm, the USBL is mounted on the support ship to estimate the real position of one I-AUV with respect to the world reference system. The acoustic modems have been used such as ideal sensors able to measure the distance among the vehicles.
The USBL transducer measures the position of a transmitting compatible modem with respect to itself [38], [39]:

$$\boldsymbol{\eta}_1^{meas,USBL} = \boldsymbol{\eta}_1 + \boldsymbol{\delta}_{\boldsymbol{\eta}_1}^{USBL} , \tag{38}$$

with added $\boldsymbol{\delta}_{\boldsymbol{\eta}_1}^{USBL}$ measurement noise. Since the measurements are obtained in spherical coordinates and then converted into Cartesian coordinates, the noise $\boldsymbol{\delta}_{\boldsymbol{\eta}_1}^{USBL}$ does not preserve the same spectral characteristic of the original sensor noise. As regards the acoustic modem feature, the S2CR 18/34 Underwater Acoustic Modem by EvoLogics is mounted on the I-AUV and it has been used for the underwater communication and for the range measurements. In the proposed study the modem is considered as a simple mean to evaluate the distance between the vehicles. The range is evaluated thanks to the measured time of flight of the acoustic wave inside the water [49], [50].
In this version of the proposed research work, random phenomena, such as failures or packet losses, have not been taken into account inside the distance estimation algorithm.

3.3.2. Xsens® MTi IMU

In the vehicle controller architecture, the Inertial Measurement Unit has been used for the estimation of the I-AUV orientation. This sensor is composed of a three-axis accelerometer, a three-axis gyroscope and a three-axis magnetometer. Each sensor has been modelled separately:

- **3D accelerometer: it measures the proper acceleration of the vehicle, minus the gravitational acceleration $\mathbf{g}_E$. This measure is then expressed in the body frame as follows:**

$$\mathbf{a}^{meas} = \left(R_b^N(\boldsymbol{\eta}_2)\right)^T (\ddot{\boldsymbol{\eta}}_1 - \mathbf{g}_E) + \mathbf{b}_a + \boldsymbol{\delta}_a , \tag{39}$$

  where $\mathbf{b}_a$ and $\boldsymbol{\delta}_a$ are, respectively, added bias and measurement noise;

- **3D gyroscope: this sensor measures the angular velocity of the vehicle in the body frame according to the following model:**

$$\boldsymbol{\nu}_2^{meas} = \boldsymbol{\nu}_2 + \mathbf{b}_{\boldsymbol{\nu}_2} + \boldsymbol{\delta}_{\boldsymbol{\nu}_2} . \tag{40}$$

  $\boldsymbol{\delta}_{\boldsymbol{\nu}_2}$ is the noise affecting the measurements, while $\mathbf{b}_{\boldsymbol{\nu}_2}$ is the sensor bias;

- **3D magnetometer: it measures the local magnetic field around the sensor, expressed in the body frame:**

$$\mathbf{m}^{meas} = W\left(R_b^N\left(\boldsymbol{\eta}_2\right)\right)^T \mathbf{H}^N + \mathbf{H}_d + \boldsymbol{\delta}_m \ . \quad (41)$$

The sensor cannot distinguish between the Earth's magnetic field $\mathbf{H}^N$ and local magnetic disturbances; hence, the model (41) takes into account the effects of Hard Iron disturbances (the added bias $\mathbf{H}_d$) and Soft Iron disturbances, scale factor and misalignment errors (matrix W) [40]. These error sources must be compensated before using the sensor. In (41), $\boldsymbol{\delta}_m$ is the sensor measurement noise.

The raw data coming from the IMU have been fused using the nonlinear complementary filter (NCF) proposed by Mahony et al. in 2008 [41]; thanks to the NCF, a reliable estimation of the orientation of the vehicle can be obtained:

$$\boldsymbol{\eta}_2^{meas} = \boldsymbol{\eta}_2 + \boldsymbol{\delta}_{\boldsymbol{\eta}_2} \ , \quad (42)$$

being $\boldsymbol{\delta}_{\boldsymbol{\eta}_2}$ measurement noise.

3.3.3. Digital Pressure Transmitter (DPT)

This sensor is vital for the operations of the I-AUVs, since it measures the local pressure according to the equation:

$$p^{meas} = p^{loc} + b_p + \delta_p \ , \quad (43)$$

where p^{loc} is the local pressure, and b_p and δ_p are added bias and measurement noise. The pressure measurement is then converted into a depth measure following the hydrostatic relation:

$$p^{meas} - p^{atm} = \rho g z^{meas} \ , \quad (44)$$

being p^{atm} the local atmospheric pressure (measured by the sensor during the initialization phase), ρ the water density and g the norm of the gravitational acceleration; hence, the measured depth can be expressed as:

$$\eta_{1z}^{meas} = z^{meas} = z + \delta_z \ , \quad (45)$$

with measurement noise δ_z. Note that the DPT added bias cancels in the subtraction (44).

3.3.4. Echosounder

The echo sounder measure is based on the SONAR (SOund NAvigation and Ranging) technique, which uses sound propagation (usually underwater, as in submarine navigation) to navigate, communicate with or detect objects on or under the surface of the water. In particular an active sonar is emitting pulses of sounds and listening for echoes. The considered device is a "low cost" single beam Ultra-Miniature Echo Sounder Imagenex 852-000-140: the considered working frequency is equal to 675 kHz, the maximum operating range is 50 m, while the transducer beam width is 10^o. In the proposed study the echo sounder is considered as a simple device to evaluate the distance from the object. To measure the distance from the object, the time from the transmission of a pulse to the reception is measured and converted into a range (by knowing the sound speed).

4. Numerical simulations and results

In this section the results of the numerical simulations are analysed. The objective of this analysis is to test the proposed cooperative strategy for a swarm of I-AUVs, highlighting its advantages and drawbacks. The simulated tasks are referred to the potential functions shown in section 2:

- Vehicle-Vehicle potential function;
- Vehicle-Object potential function;
- Vehicle-Environment potential function.

The sum of all these contributes determines the I-AUVs swarm trajectory. The analysed task is a classical transportation task, guided by the ROSV, in which the swarm is composed by 4 I-AUVs. The transportation phase is performed in an environment with two obstacles disposed along the desired trajectory. Each vehicle has a single robotic arm with 7 DOFs and a gripper that is (for hypothesis) rigidly connected with the object. The simulation environment is MATLAB®- Simulink®and the used integrator is the fixed step ODE 5 Dormand-Prince with a step-size of $\Delta t = 1e^{-4}$ s. The authors have shown the preliminary results into a video.

4.1. Cooperative manipulation with obstacle avoidance phase

In this section, the preliminary results of the cooperative manipulation with obstacle avoidance are shown. The cooperative mobile manipulation is performed by 4 I-AUVs placed at the four corners of the object. The obstacles are modelled as spheres (2 m radius). The robotic arms started from an initial position computed by the inverse differential kinematics algorithm to avoid singularity positions. In Figure 15, the initial positions of the vehicles are represented; in addition, the influence areas of the potentials are shown (the red circle is the Vehicle-Obstacle potential and the green circle is the Vehicle-Vehicle one). The red line is the desired trajectory of the swarm given by the ROSV and the red dotted one is the supposed .

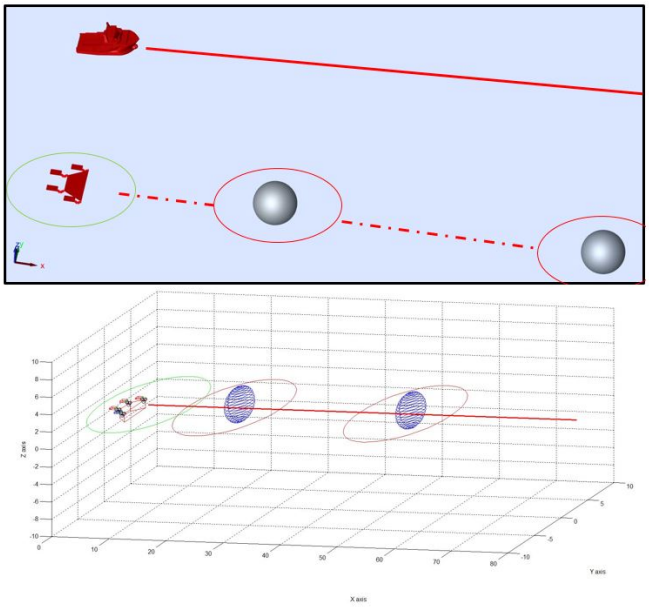

Figure 15: Initial conditions of the I-AUVs swarm, showing the object, the obstacles and the influence areas

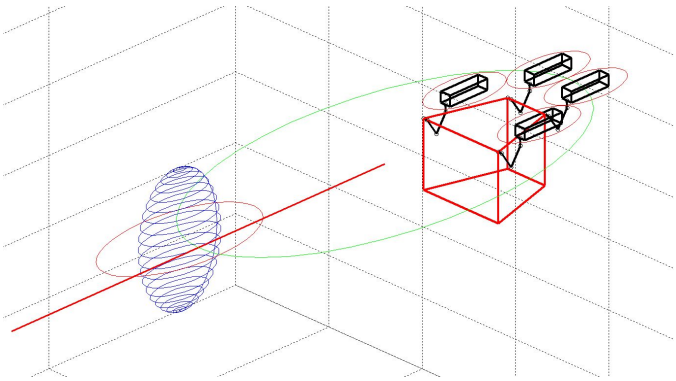

Figure 16: Zoom on the initial conditions of the I-AUVs swarm with the influence areas

Figure 16 shows a zoom of the initial poses of the vehicles, where we can clearly see the other different interactions: the green circle (Vehicle-Vehicle interaction) and the red one (Vehicle-Obstacle interaction).

Figures 17 to 20 describe the dynamical behaviour of each vehicle in presence of both the obstacles and the object in terms of x, y, z and of α, β, ψ. It is worth noting the effects of the obstacle presence: the obstacle avoidance phases are quite smooth,but able to simultaneously maintain the swarm formation.

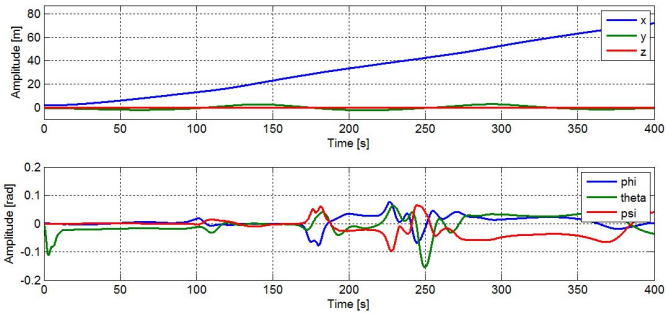

Figure 17: Vehicle 1: position and orientation

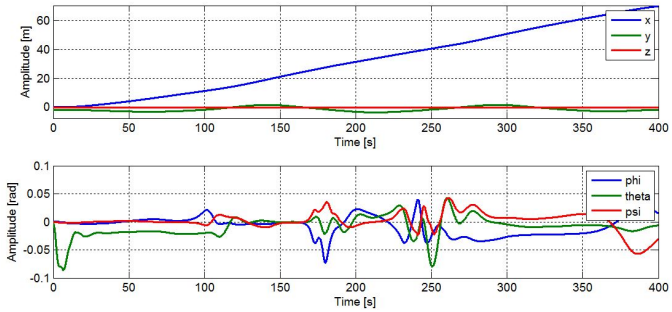

Figure 18: Vehicle 2: position and orientation

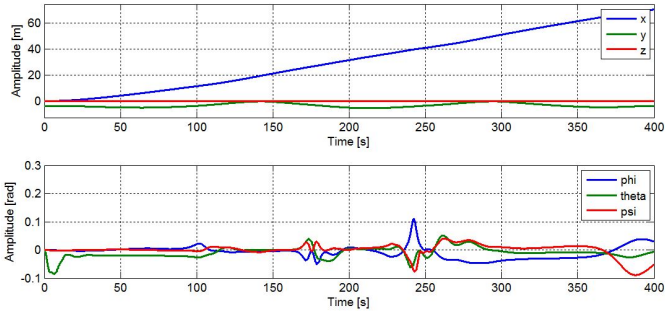

Figure 19: Vehicle 3: position and orientation

In Figure 21, the total force acting on the vehicle 1 is shown. The total force consists of different contributions

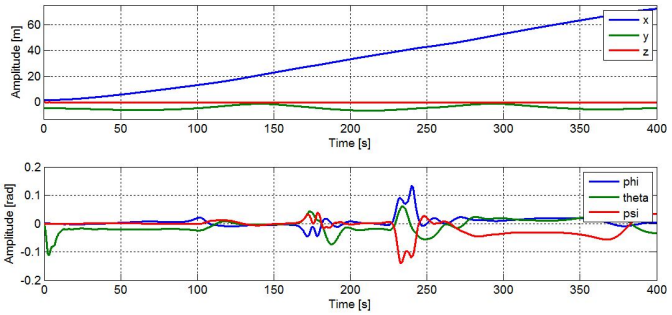

Figure 20: Vehicle 4: position and orientation

due to the Vehicle-Vehicle, Vehicle-Object and Vehicle-Environment potentials. In the figures, the forces, for sake of clarity, are expressed in the world reference frame. Figures 22-26 represent the contributions of each potential action acting on the I-AUV. It is interesting to note that the most important contribution is related to the attractive potential of the swarm V^{swarm} (Figure 22). This contribution is supported by the $V^{polygon}$ to maintain the swarm in formation (the force in Figure 23 is quite constant because the potential maintains constant the distance during the task) and by the $V^{collisions}$ which prevents the collisions among the I-AUVs. Since the formation is kept during the whole task, the force shown in Figure 24 is nearly zero. The Vehicle-Object potential (related to the two contributions V^{WS} and V^{RAcoll}) is not here reported because the forces related to these potentials are zero. The reason is that the robotic arm controller presents good performance in terms of stability and robustness by maintaining the I-AUV end-effector pose in the predefined pose. Finally, the presence of the obstacles along the path alters the predefined straight trajectory of the swarm due to the actions of the Vehicle-Environment potentials V^{v-e} (shown in Figures 25-26).

For sake of synthesis, the authors have reported only the forces acting on the Vehicle 1, but the swarm motion is obviously influenced by the contributions of all the vehicles.

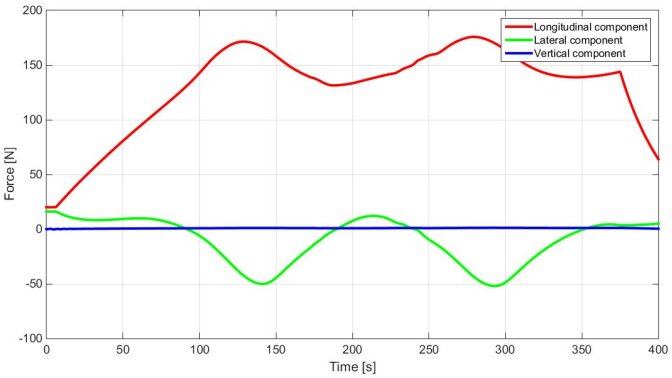

Figure 21: Vehicle 1: total force due to the potential interactions

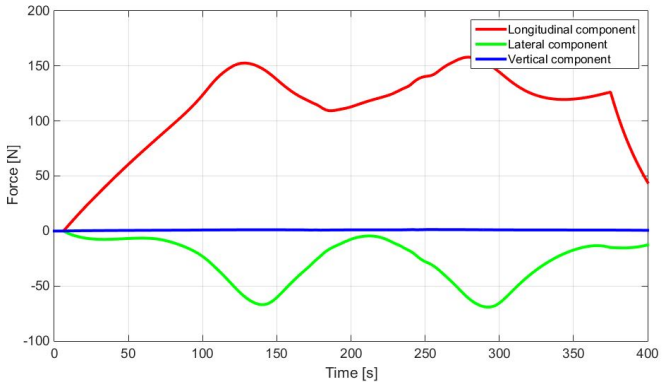

Figure 22: Vehicle 1: force due to the V^{swarm}

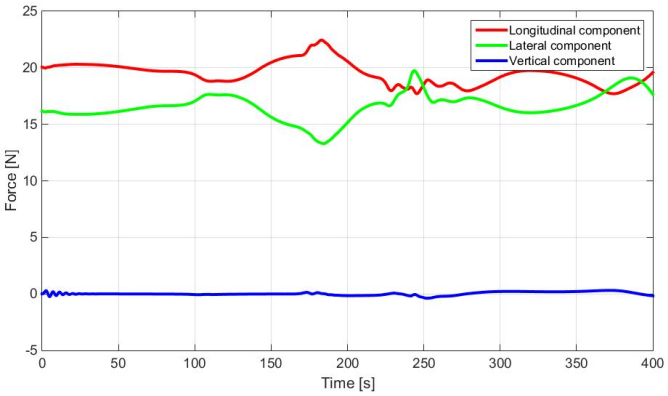

Figure 23: Vehicle 1: force due to the $V^{polygon}$

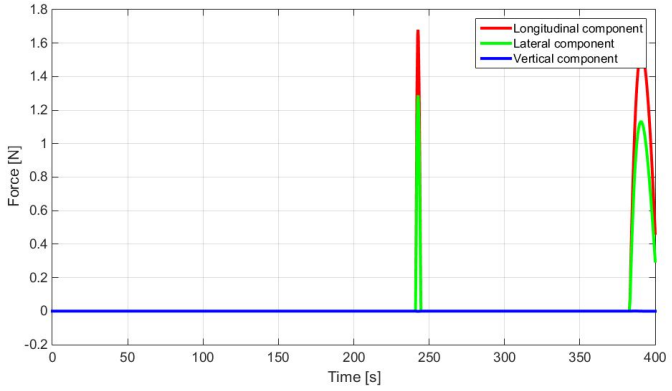

Figure 24: Vehicle 1: force due to the $V^{collisions}$

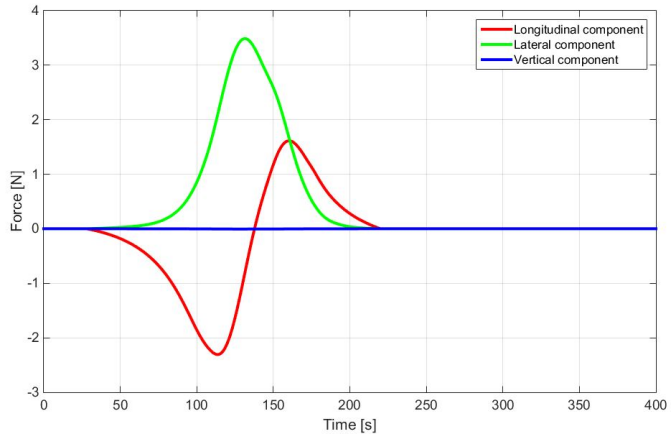

Figure 25: Vehicle 1: force due to the V^{v-e} potential related to the first obstacle

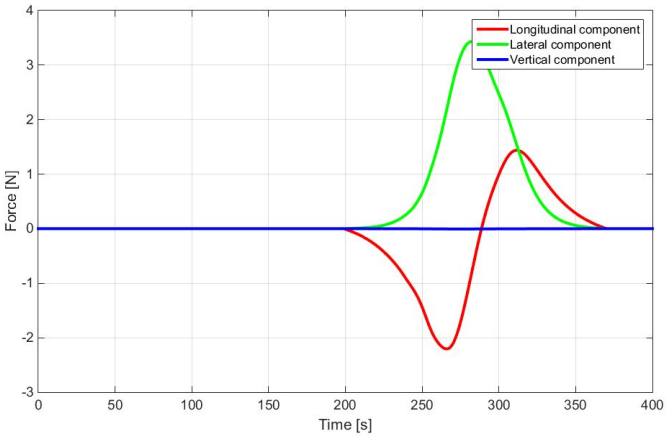

Figure 26: Vehicle 1: force due to the V^{v-e} potential related to the second obstacle

In conclusion, Figure 27 represents the final condition of the I-AUVs swarm, after the obstacle avoidance phases in which the object is carried by the swarm; in addition, in Figure 28 the trajectories of the vehicles in the xy plane are shown. At the end of the simulation, the vehicles reached the swarm desired position (the green circle), showing the good capacities of the control approach.

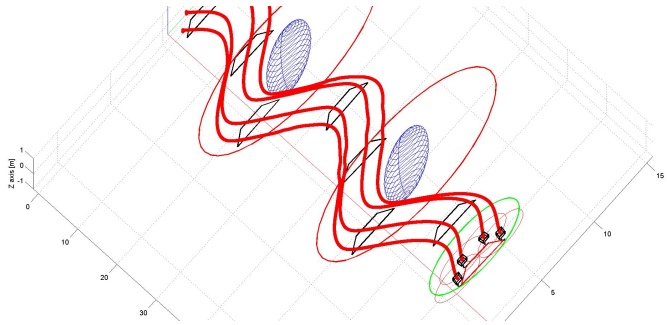

Figure 27: Final conditions of the I-AUVs swarm (3D trajectories)

5. Conclusions and future developments

The development of different control architectures for cooperative mobile manipulation represents a challenging field of autonomous robotics, especially in the underwater environment. In such systems, the main advantage regards the possibility to perform complex and dexterous tasks which cannot be simply made using a single manipulator: for instance, multiple cooperative manipulators can be used to move objects, action that cannot be performed by a single robot (due to the object size and weight constraints). The study of cooperative manipulation strategies of Intervention-Autonomous Underwater

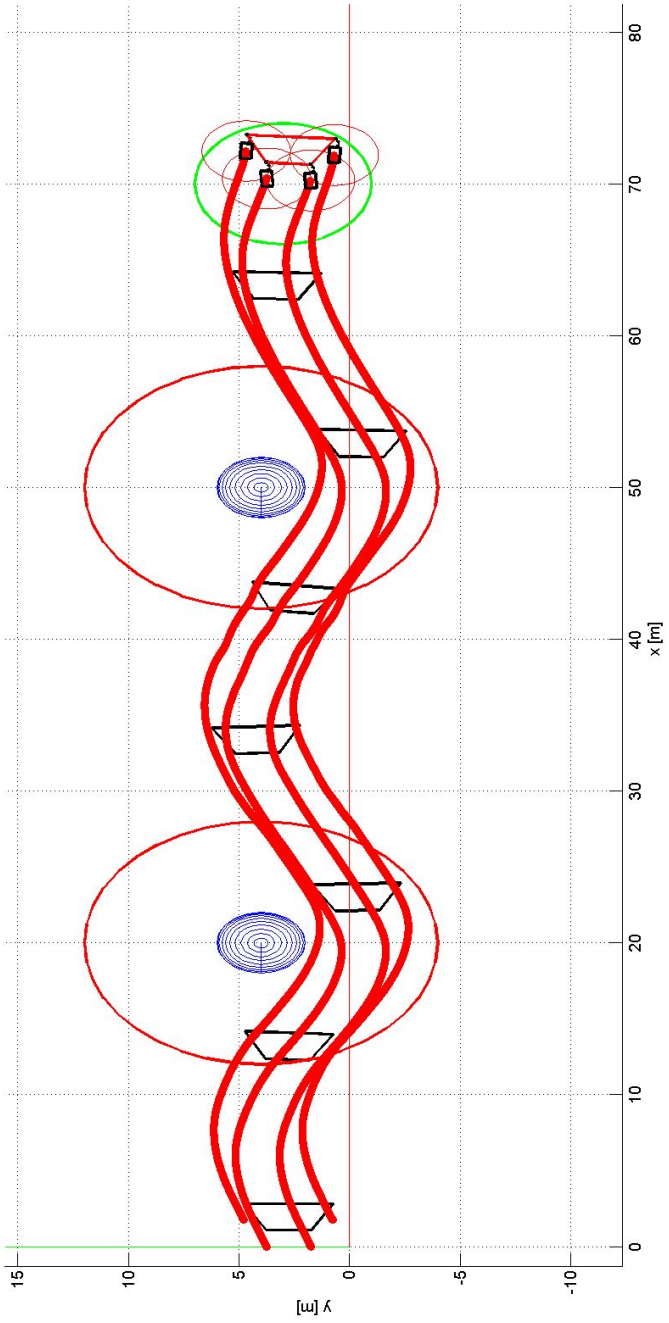

Figure 28: Final conditions of the I-AUVs swarm (2D trajectories - XY plane)

Vehicles (I-AUVs) represents a more complex field of application, compared to the terrestrial or aerial ones, both due to different technological problems, e.g. localization and communication in underwater environment. In this paper, the authors proposed an innovative decentralized approach for cooperative mobile manipulation of I-AUVs. This decentralized strategy is based on a different use of potential field method; particularly, a multi-layer control structure is developed to in parallel manage the coordination of the swarm, the guidance and navigation of I-AUVs and the manipulation tasks. This modular architecture can be applied to manage both navigation phases and manipulation ones; in particular, in this paper, the authors developed the strategy for a transportation phase. The multi-layer control structure controls both the swarm, the vehicle and the robotic arm motion and the main layers deal with Vehicle-Vehicle, Vehicle-Environment and Object-Environments interactions respectively. **Due to the current gap between the real operations of the AUV and the future cooperative mobile manipulation of I-AUVs, the authors proposed to evaluate the cooperative manipulation strategy only in terms of numerical simulations.** As shown along the paper, the main advantages of the potential field method were the reduced number of exchanged data and the homogeneity of the approach; in fact, navigation and control problems are reduced to the individuation of the distance vector among the vehicles, object and obstacles. The approach permits the reduction of the on board sensors, reducing the whole vehicle complexity and, because of the technological problems caused by the underwater environment, the reduction of the transmitted data is one of the keypoints of this architecture to perform underwater operations with low bandwidth. The innovative concept behind the distance estimation algorithm (the only quantities necessary to perform control actions and uniquely measured by on board sensors) is to use the object to be manipulated (supposed known a priori) such as the swarm reference system and the surface vehicle only as the connection point with the world reference system. This way, the architecture allows the use of acoustic modems rather than expensive Ultra Short Base Line (USBL) system. **The authors, thanks to experience acquired in previous research activities [42], [45], [46], [47], [43], [44], [48] in the AUV field, have modelled the typical behaviour of the sensors (e.g. Inertial Measurement Unit, acoustic modem, gyroscopes, etc..) to better investigate the accuracy of the method with respect to the sensors performances.**
In the numerical simulation results, the authors performed several simulations to test the control strategy based on the potential field method: the I-AUV swarm is composed of 4 vehicles, each one provided of a 7 Degree Of Freedoms (DOFs) robotic arm. The simulation scenario shown in this paper is a very interesting one in where the swarm has to move a known object in an unknown environment, e.g. a harbour; particularly, the manipulation task is to

carry the object along a known trajectory (transmitted by an external vehicle, e.g a surface vehicle) and where some obstacles are placed. The results are very encouraging because the I-AUVs swarm keeps both the formation during the manipulation phase and the object during an avoiding manoeuvre performed due to the presence an obstacle with smoother trajectories.

In spite of the gap between real scenarios and the development of I-AUV swarm, the future developments planned for this research activity will be the implementation of more realistic models describing random phenomena of the acoustic communication, such as failures or packet losses, during the estimation of the distance among I-AUVs. Furthermore, a deeper investigation on different solutions for the optimal tuning of the potential gains will be performed as well. Finally, thanks to swarm of AUVs developed and built by the MDM Lab of the University of Florence [42], [43], some preliminary tests regarding the proposed control architecture based on potential field method will be carried out.

References

[1] F. Bullo, J. Cortes, and S. Martinez. *Distributed Control of Robotic Networks*. Princeton University Press, 2008.

[2] R. Olfati - Saber, J.A. Fax, and R.M. Murray. *Consensus and cooperation in networked multi-agent systems*. Proceedings of the IEEE, 95(1), pp. 215-233, 2007.

[3] Siciliano B., Khatib O., *Handbook of Robotics*, Springer Handbooks, Napoli and Stanford, 2008.

[4] O. Khatib, K. Yokoi, K. Chang, D. Ruspini, R. Holmberg, and A. Casal, *Vehicle/Arm Coordination and Multiple Mobile Manipulator*, Intelligent Robots and Systems, pp. 546 - 553 vol.2, 1996.

[5] H. G. Tanner, S. Loizou, and K. J. Kyriakopoulos, *Nonholonomic navigation and control of cooperating mobile manipulators*, IEEE Trans. Robot. Autom., vol. 19, no. 1, pp. 53 – 64, Feb. 2003.

[6] T. Tarn, G. Shoults. and S. Yang, *A dynamic model of an underwater vehicle with a robotic manipulator using kane method*, Autonomous Robots, pp. 195 - 282, 1996.

[7] Jianan Wang, Ming Xin*Distributed optimal cooperative tracking control of multiple autonomous robots* Robotics and Autonomous Systems, Volume 60, Issue 4, April 2012, Pages 572-583, ISSN 0921-8890.

[8] G. Antonelli, *Underwater Robots*, Springer Tracts in Advanced Robotics, Springer-Verlag, 2nd edition, Heidelberg, 2006.

[9] G. Shoults, *Dynamics and Control of an Underwater Robotic Vehicle with an N-axis Manipulator*, Washington University: Ph.D Thesis, 1996.

[10] J. Kim, W. K. Chung, and J. Yuh, *Dynamic analysis and two-time scale control for Underwater vehicle manipulator systems*, in IEEE/RSJ Int. Conf on Intelligent Robots and Systems, Vol. 1. pp. 577 - 582, 2003.

[11] G. Antonelli, F. Caccavale, S. Chiaverini, and L. Villani, *Tracking control for underwater vehicle manipulator systems with velocity estimation*, IEEE Journal of Oceanic Engineering, vol. 25, no. 3, pp. 399-413, 2000.

[12] Y. Cui and N. Sarkar, *A unified force control approach to autonomous underwater manipulation*, Robotica, vol. 19, pp. 255-266, 2001.

[13] Y. Cui and J. Yuh, *A unified adaptive force control of underwater vehicle-manipulator systems (uvms)*, IEEE/RSJ Int. Conf on the Intelligent Robots and Systems,pp. 553-558, 2003.

[14] G. Antonelli, S. Chiaverini, *Fuzzy redundancy resolution and motion coordination for underwater vehicle-manipulator systems*, IEEE Transactions on Fuzzy Systems, vol. 11, no. 1, pp. 109-120, 2003.

[15] N. Sarkar and T. K. Podder, *Coordinated motion planning and control of autonomous underwater vehicle-manipulator systems subject to drag optimization*, IEEE Journal of Oceanic Engineering, vol. 26, no. 2, pp. 228 - 239, 2001.

[16] C. C. de Wit, E. O. Diaz, and M. Perrier, *Control of an underwater vehicle manipulator with composite dynamics*, Proc. of the American Control Conference,(Philadelphia, Pennsylvania), pp. 389-393, 1998.

[17] Y. Hirata, Y. Kume, T. Sawada, Z.Wang, and K. Kosuge, *Handling of an object by multiple mobile manipulators in coordination based on casterlike dynamics*, Proc. IEEE Int. Conf. Robot. Autom., vol. 26, pp. 807 – 812, 2004.

[18] Thomas G. Sugar and Vijay Kumar, *Vehicle/Arm Coordination and Multiple Mobile Manipulator*, IEEE Transactions on Robotics and Automation, vol. 18, no. 1, pp. 94-103, 2002.

[19] T.I. Fossen, *Guidance, Navigation and Control of Ocean Vehicles*, 1st edition, Chichester, UK: John Wiley&Sons, 1994.

[20] M. Breivik, and T.I. Fossen, *Guidance-Based Path Following for Autonomous Underwater Vehicles*, in Proc. of OCEANS 05, Washington D.C., USA, 2005.

[21] A. Bahr and J. Leonard, *Cooperative localization for autonomous underwater vehicles*, Proc. 10th International Symposium on Experimental Robotics (ISER), Rio de Janeiro, Brazil, July 2006.

[22] *Remotely operated vehicles of the world*, SMD Hydrovision, Seventh edition, 2006.

[23] International Standard ISO 13628-8, *Part 8: Remotely Operated Vehicle (ROV) interfaces on subsea production systems*, ISO 2002.

[24] F. Cheli, E. Pennestri, *Kinematics and dynamics of multibody systems*, CEA, 2009.

[25] *Official site of Mathworks*, www.mathworks.com, 2013.

[26] M. Morgado, P. Oliveira, C. Silvestre, J.Fernandes Vasconcelos; *Embedded Vehicle Dynamics Aiding for USBL/INS Underwater Navigation System*. Control Systems Technology, IEEE Transactions on. Volume: 22 , Issue: 1-2014. pp: 322 – 330.

[27] Allotta B, Costanzi R, Meli E, Pugi L, Ridolfi A, Vettori G. *Cooperative localization of a team of AUVs by a tetrahedral configuration*. Robotics and Autonomous Systems. 2014.

[28] A.Caiti, V. Calabro, T. Fabbri, D. Fenucci, A. Munafo; *Underwater communication and distributed localization of AUV teams*. OCEANS - Bergen, 2013 MTS/IEEE. DOI: 10.1109/OCEANS-Bergen.2013.6608166 pp:1-8.

[29] TRIDENT EU project, FP7-ICT Challenge 2: Cognitive Systems, Interaction, Robotics Collaborative Project (STREP), Grant agreement No: ICT-248497. http://www.irs.uji.es/trident/.

[30] PANDORA EU project, FP7-ICT STREP research project, Challenge 2: Cognitive Systems, Interaction, Robotics Collaborative Project. On going project. http://persistentautonomy.com.

[31] Xue Qi *Adaptive coordinated tracking control of multiple autonomous underwater vehicles*, Ocean Engineering 91, 2014, pp.88-90.

[32] Gao Yun; Wei Zhiqiang; Gong Feixiang; Yin Bo; Ji Xiaopeng, *Dynamic Path Planning for Underwater Vehicles Based on Modified Artificial Potential Field Method* Digital Manufacturing and Automation (ICDMA), 2013 Fourth International Conference on , vol., no., pp.518,521, 29-30 June 2013.

[33] Saing Paul Hou; Chien-Chern Cheah, *Can a Simple Control Scheme Work for a Formation Control of Multiple Autonomous Underwater Vehicles?* Control Systems Technology, IEEE Transactions on , vol.19, no.5, pp.1090,1101, Sept. 2011.

[34] Stilwell, D.J.; Bishop, B.E.; Sylvester, C.A. *Redundant manipulator techniques for partially decentralized path planning and control of a platoon of autonomous vehicles* Systems, Man, and Cybernetics, Part B: Cybernetics, IEEE Transactions on , vol.35,

no.4, pp.842,848, Aug. 2005

[35] Allotta B., Caiti A., Chisci L., Costanzi R., Di Corato F., Fantacci C., Fenucci D., Meli E., Ridolfi A., *Development of a Navigation Algorithm for Autonomous Underwater Vehicles*, in Proceedings of the IFAC Workshop on Navigation Guidance and Control of Underwater Vehicles (NGCUV 2015), Girona, Spain (2015).

[36] Allotta B., Bartolini F., Costanzi R., Monni N., Pugi L., Ridolfi A., *Preliminary design and fast prototyping of an autonomous underwater vehicle propulsion system*, in Proceedings of the Institution of Mechanical Engineers, Part M: Journal of Engineering for the Maritime Environment, Jan. 27 (2014); DOI 10.1177/1475090213514040.

[37] University of Wisconsin, Green Bay website: *http://www.uwgb.edu*

[38] Larsen M., *Synthetic Long Baseline Navigation of Underwater Vehicles*, in Proceedings of MTS/IEEE OCEANS 2000, Providence, RI, USA (2000).

[39] Rigby P., Pizarro O., Williams S., *Towards Geo-referencing AUV Navigation Through Fusion of USBL and DVL Measurements*, in Proceedings of MTS/IEEE OCEANS 2006, Boston, MA, USA (2006).

[40] VectorNav Technologies: *http://www.vectornav.com*

[41] Mahony R.E., Hamel T., Pflimlin J.M., *Nonlinear Complementary Filters on the Special Orthogonal Group*, IEEE Trans. on Automatic Control, Vol. 53, N. 5, pp 1203-1218 (2008).

[42] THESAURUS project, *http://thesaurus.isti.cnr.it/*

[43] FP7 ARROWS European project, *http://www.arrowsproject.eu/*

[44] B. Allotta, R. Costanzi, A. Ridolfi et al., *The ARROWS project: adapting and developing robotics technologies for underwater archaeology,* in IFAC Workshop on Navigation Guidance and Control of Underwater Vehicles (*NGCUV*2015), Girona, Spain, April 2015.

[45] B.Allotta, L.Pugi, F.Bartolini, R.Costanzi, A.Ridolfi, N.Monni, J.Gelli, G.Vettori, *The THESAURUS project, a long range AUV for extended exploration, surveillance and monitoring of archaeological sites,* V International Conference on Computational Methods in Marine Engineering, ECCOMAS MARINE 2013, Hamburg, Germany, May 2013.

[46] B. Allotta, R. Costanzi, E. Meli, L. Pugi, A. Ridolfi, G. Vettori, *Cooperative Localization of a Team of AUVs by a Tetrahedral Configuration* Robotics and Autonomous Systems, Elsevier, vol.62, pp 1228,1237 (2014).

[47] Allotta, B., Pugi, L., Bartolini, F., Ridolfi, A., Costanzi, R., Monni, N., Gelli, J., *Preliminary Design and Fast Prototyping of an Autonomous Underwater Vehicle Propulsion System.* In Proceedings of The Institution of Mechanical Engineers, Part M, Journal of Engineering for the Maritime Environment, d.o.i. 10.1177/1475090213514040 (online January 2014).

[48] B.Allotta, R.Conti, R.Costanzi, F.Giardi, E.Meli, A.Ridolfi, *Modelling and Control of an Autonomous Underwater Vehicle for Mobile Manipulation.* Multibody Dynamics 2013 Congress (ECCOMAS 2013), Zagreb, Croatia, 1-4 July 2013.

[49] D. De Palma, G. Indiveri, G. Parlangeli, *Multi-vehicle relative localization based on single range measurements*, 3rd IFAC Workshop on Multivehicle Systems 2015, Genova, Italy.

[50] F. Arrichiello, G. Antonelli, A.P. Aguiar, A. Pascoal, *Observabiliy metrics for the relative localization of AUVs based on range and depth measurements: theory and experiments.* In Proceedings of the 2011 IEEE/RSJ International Conference on Intelligent Robots and Systems, IEEE-IROS 2011. San Francisco, CA, USA.